energies

MDPI

*Review*

# An Overview of Permanent Magnet Generator Architectures and Control for Wave Energy Conversion Systems

**Bhavana Mudigonda [1,*], Giacomo Moretti [2] and Elisabetta Tedeschi [1,2]**

[1] Department of Electric Energy, Norwegian University of Science and Technology (NTNU), 7034 Trondheim, Norway; elisabetta.tedeschi@ntnu.no
[2] Department of Industrial Engineering, University of Trento, 38123 Trento, Italy
* Correspondence: bhavana.mudigonda@ntnu.no

## Abstract

Wave energy is gaining momentum as a viable and environmentally sustainable source of renewable power, with the potential to contribute significantly to the global energy mix. Central to wave energy conversion is the power take-off system, where electromagnetic generators play a crucial role in determining overall system performance, reliability, and efficiency. This paper provides a review of wave energy conversion devices and classifies the main power take-off mechanisms. It evaluates and compares key generator types based on their performance under wave energy conditions. Among these, Permanent Magnet Synchronous Generators have demonstrated strong potential due to their high efficiency, power density, and suitability for low-speed direct drive configurations typical of wave environments. The review presents a detailed analysis of advanced permanent magnet generator topologies, focusing on structural designs, control methods, and wave-specific trade-offs. It also investigates hierarchical control strategies, where high-level decisions are based on wave conditions and low-level control ensures accurate generator operation. The paper aims to provide a broad perspective on the design and control of electromagnetic generators for wave energy systems.

**Keywords:** wave energy conversion; power take-off; electromagnetic generator; generator control; Permanent Magnet Synchronous Generator; linear permanent magnet generator

## 1. Introduction

The wave energy market is expected to grow at a yearly rate of ∼4% until 2030 [1], if properly underpinned by wave energy conversion technological development. To meet the demands of this growing sector, it is essential to design and control wave energy converters (WECs) capable of delivering high efficiency at high power density while ensuring reliability and economic viability for large-scale deployment.

Central to this challenge is the design and control of the electro-magnetic generator (EMG) [2,3], which is an important component of a wave energy converter's power take-off (PTO) system [4–6]. The PTO extracts mechanical energy from the wave induced motion and converts it into electrical energy, with the EMG impacting the efficiency, controllability and overall techno-economic performance of the conversion process. Advanced generator topologies [7–10] and integrated control strategies [11–14] are particularly important in this context, as they enable compact, high-torque-density architectures [15] with fewer



Academic Editor: Duarte Valério

Received: 19 May 2025
Revised: 15 December 2025
Accepted: 21 December 2025
Published: 26 December 2025

mechanical components, reduce capital and maintenance costs [16], and support efficient grid integration [17], all of which are critical for accelerating commercial deployment [18] of WECs.

Unlike other renewable sources, wave energy features strongly fluctuating and bidirectional input power, with low frequency variability (∼0.1 Hz) and a high peak-to-average ratio. These characteristics (Figure 1) impose demanding operational requirements on generators, including wide-ranging speed capability, bidirectional and low-speed operation, and high torque density within compact volumes. Operating in harsh marine conditions further complicates WEC development as components must withstand cyclic and bidirectional loading, corrosion, biofouling, and limited maintenance access [19,20].

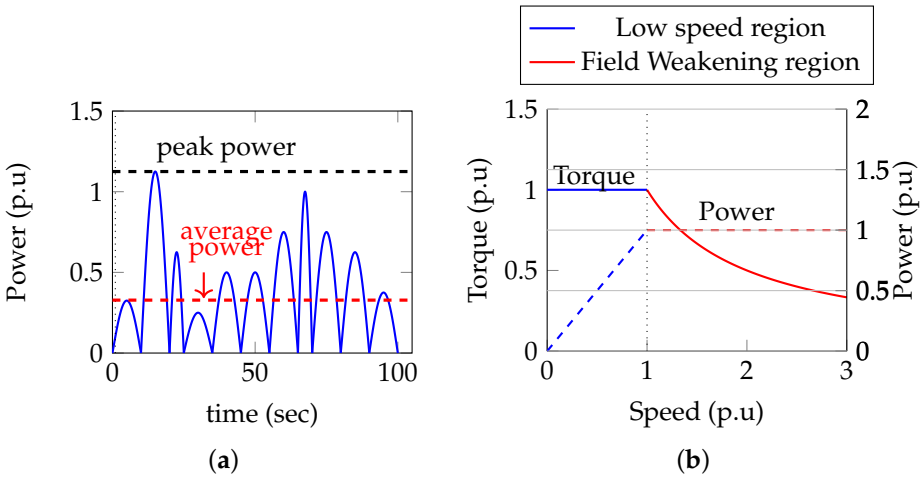


**Figure 1.** Typical power input and torque–speed characteristics of an EMG for WEC systems. (**a**) Example of mechanical input power to an EMG, normalized to its rated output power, adapted from [21]. (**b**) Torque-speed (solid line) and power-speed (dashed line) characteristics of a Permanent Magnet Synchronous Generator (PMSG), adapted from [22].

Existing studies have examined electrical generators for wave energy and other low-speed applications from various perspectives. Broad reviews [23] summarize progress across electromagnetic, piezoelectric, and triboelectric concepts, offering useful context but providing limited analysis of PMSGs. Low speed permanent magnet machines developed for wind [24] and marine current turbines [25] offer valuable analogies but do not fully account for the specific working conditions of WECs. More focused analyses have explored specific generator families, including interior, surface-mounted, V-shaped, and PM-assisted synchronous reluctance machines, highlighting differences in torque density, efficiency, and constructional complexity [26]. Axial flux modulation generators have also been investigated for linear-rotary systems [27], demonstrating compact PTO integration but noting manufacturing and control challenges. Similarly, flux-switching machines have been reviewed for their modularity and high power density [28], yet limited attention has been paid to their performance under realistic wave-specific operating conditions. The joint influence of generator design choices and control under realistic WEC operating conditions is relatively underexplored. Collectively, these studies highlight that, although the diversity of generator topologies is well documented, design choices have rarely been considered in combination with control strategies under stochastic WEC loading, and an assessment of their performance under realistic wave conditions is still lacking.

This paper presents a review of PMSG technology specifically tailored to the working conditions of wave energy systems. A comparison of the requirements of PMSGs for WECs, wind, and tidal systems is presented, clarifying how WEC operating conditions differ

from those of other renewable energy technologies. Qualitative comparisons of different generator topologies and winding configurations are presented and are complemented by available quantitative performance data to support the evaluation.

Unlike previous reviews in this field, this paper consolidates PMSG design adaptations and control strategies into a unified framework tailored to WEC conditions.

The guiding research questions of this literature review are as follows: (i) How do WEC operating conditions affect generator requirements? (ii) Which machine architectures and design configurations better meet these design requirements in the marine environment? (iii) How can generator-level control be coordinated with system-level strategies to improve WEC performance?

The article is structured as follows: Section 2 presents an overview of WEC devices and corresponding PTO systems. Section 3 reports a technological review of EMGs for wave energy applications. Section 4 focuses on PMSM topologies and design specifications. Section 5 focuses on high-level and generator-level control strategies, and Section 6 draws conclusions.

## 2. Overview of Wave Energy Conversion Devices and Power Take-Off Systems

The conversion of ocean wave energy into electricity involves two key components: the prime mover (or WEC device) and the PTO system. The prime mover captures the oscillatory motion of ocean waves and transforms this motion into mechanical energy at the input of the EMG, using single/multiple stages depending on the PTO architecture. Once the mechanical energy reaches the EMG, it is converted into electrical energy. However, due to the fluctuating nature of wave-induced motion, the electrical output from the EMG is typically irregular and varies in both frequency and amplitude. To address these variations and ensure compatibility with grid requirements, power electronic converters configured as back-to-back converters are employed. These consist of a machine side converter (MSC) and a grid side converter (GSC), connected through a DC link. The MSC regulates the operation of the EMG, while the GSC ensures that the regulated electrical energy is delivered to the grid.

### *2.1. Types of WEC Technologies*

The primary conversion stage can be implemented based on different operational principles as listed, each employing a distinct method to harness wave energy, thereby influencing the design and control of the PTO and the overall power conversion system. Oscillating water column devices consist of an air chamber with a submerged water inlet. As the wave approaches, the water is pushed into the chamber, transferring the wave energy to the air above the water surface [29]. The energy from the compressed air propels a bidirectional turbine. Oscillating-body devices are mechanical structures that oscillate with waves, converting the wave energy into potential/kinetic energy of the oscillating body. The devices are called surging [30,31], pitching, or heaving devices [32] based on their motion relative to the free surface, and they can consist of multibody articulated structures [33]. Overtopping devices capture the water that spills over the device with the movement of the waves and use the stored water to drive a low-head turbine [34]. Pressure differential devices generate power leveraging the movement of flexible structures (e.g., membranes or diaphragms) to capture the energy from the waves [35–37].

### 2.2. PTO Architectures

This section reviews the main types of PTO architectures used in WECs (Figure 2), highlighting their design principles, operational characteristics, and typical WEC devices used for each architecture. Hydraulic Circuit PTOs use mechanical energy from a WEC device (typically an oscillating body) to drive a hydraulic system that pressurizes a working fluid within a circuit. The pressurized liquid is further directed to a hydraulic turbine or motor to convert the hydraulic energy into rotational mechanical energy to drive the EMG. An accumulator may be included to reduce the variability of power output [38,39].

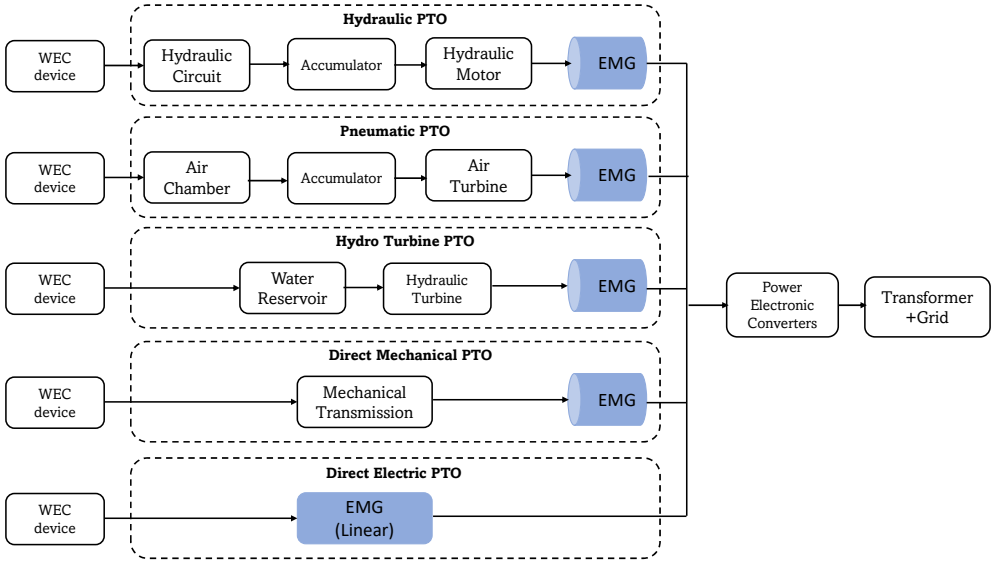


**Figure 2.** Typical PTO architectures.

Pneumatic PTOs utilize the mechanical energy from the WEC device, such as an oscillating wave column or submerged pressure differential devices, to drive a pneumatic system to induce compression or expansion of the air in a chamber and feed an air turbine connected to an EMG. The pneumatic PTO can also include an accumulator that temporarily stores compressed air to smooth the power output [40]. Hydraulic turbine PTOs harness the wave energy as gravitational potential energy stored in a water reservoir. The stored water flows through a hydraulic turbine that drives an EMG. The primary WEC device for this configuration is the overtopping device [41].

Direct-mechanical drive PTOs feature a configuration in which a WEC device, such as an oscillating body, converts wave energy into mechanical energy. A mechanical transmission (e.g., a gearbox) is then used to adapt the speed and mechanical load requirements for the generator [23]. This configuration allows the use of traditional rotational machines, as the wave's low-speed input is typically converted to high-speed rotary motion via the mechanical transmission. However, the electric generator is continuously subjected to power and torque oscillations, as variations in the wave input are directly reflected at the generator's input. To address these issues, several works propose incorporating a mechanical motion rectifier (MMR) within the mechanical transmission stage. MMRs use one-way clutches and geared transmissions to convert the bidirectional motion from the WEC into a unidirectional rotational output. For example, ref. [42] integrates two one-way bearings into a rack–pinion system to convert the oscillating motion into forward-only rotation. Ref. [43] uses three bevel gears and two one-way clutches that allow rotational motion to pass in only one direction. Similarly, ref. [44] employs one-way clutches, gears, and a ball screw to rectify the bidirectional input. When combined with a flywheel, these

MMR configurations can provide a smoother rotational profile, reduce mechanical fatigue caused by frequent reversals, and offer a more stable input to the generator. This smoother and unidirectional operation also leads to more reliable power converter performance, since reduced speed fluctuation results in smaller junction-temperature variations [44]. However, the main drawbacks of MMRs are the increased mechanical complexity and the additional losses and wear introduced by the additional clutches, gears, and rotating components.

Direct-electric drive PTOs are similar to direct-mechanical drive PTOs, except that they use the WEC motion or deformation to directly drive a generator (e.g., linear EMG, electroactive polymer membranes [45], and magnetic geared machines [46]) without any mechanical transmission. These systems generate electrical energy in a single stage, thereby eliminating intermediate energy conversion stages that are often sources of inefficiency. The removal of intermediate mechanical stages also offers benefits such as reduced maintenance costs, lower downtime, and improved lifetime and reliability of the WEC. Furthermore, they enhance the overall controllability of a WEC, enabling the implementation of more effective control strategies for EMGs to maximize energy harvesting. Generators in such systems require a large number of poles to generate high power at low rotational speeds. Using magnetically geared machines reduces mechanical complexity and maintenance issues associated with conventional gears, while potentially allowing for a more compact generator design [47].

## 3. EMG Technologies for WEC Systems

The generators within the PTO system convert mechanical energy into electrical energy. Among the various PTO configurations, hydraulic circuits, pneumatic systems with accumulators, and hydraulic turbine PTOs allow the generator, which is typically rotary, to operate at a fixed speed. In contrast, direct-mechanical drive PTOs use a variable-speed rotary generator, while direct-electric drive PTOs typically use a linear generator with variable-speed operation.

### *3.1. Overview of EMG Types*

Considering all PTO configurations, the generators employed for wave applications include induction generators (IGs), Permanent Magnet Synchronous Generators (PMSGs), and Synchronous Reluctance Generators (SRGs). These generators can be either rotary (Figure 3) or linear (Figure 4). This section offers an overview of the construction, operation, advantages, and disadvantages of each generator type, and compares their performance based on the key metrics essential for choosing a generator for wave converters.

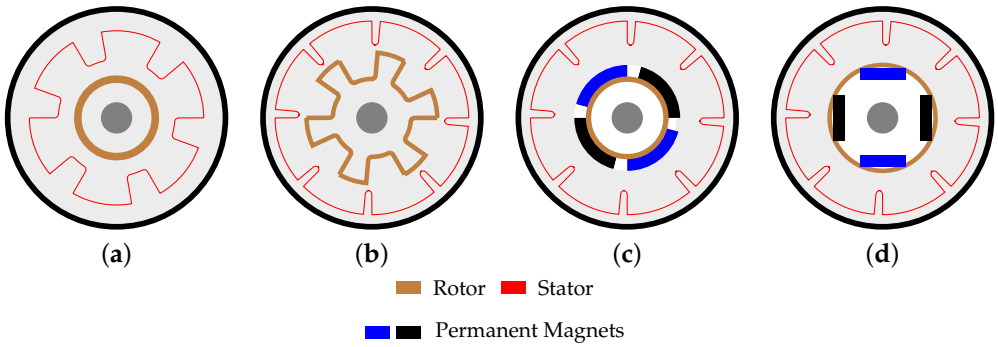


**Figure 3.** Structure of rotary generator topologies used in WECs. (**a**) Induction generator; (**b**) Switched Reluctance Generator; (**c**) Permanent Magnet Synchronous Generator (surface mount); (**d**) Permanent Magnet Synchronous Generator (interior).

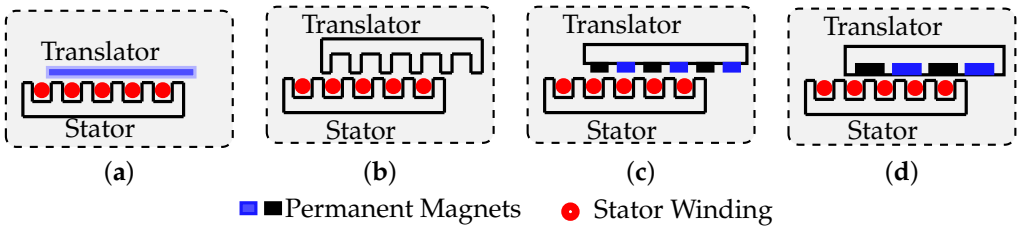


**Figure 4.** Structure of Linear Generators. (**a**) Linear IG; (**b**) Linear SRG; (**c**) PMSG (surface); (**d**) PMSG (interior).

#### 3.1.1. Induction Generators

Induction generators (IGs) (Figures 3a and 4a) are well-known for their robustness, reliability, and cost-effectiveness. They are considered workhorses in many industries, and their control techniques are well established and easy to use, even for wave applications. Among them, the squirrel cage induction generator (SCIG) is widely used due to its simplicity and low maintenance requirements, while the doubly-fed induction generator (DFIG) offers greater control flexibility and efficiency, making it suitable for variable-speed applications. A DFIG allows more control over the generator's speed and torque by accessing both stator and rotor terminals. The advantage of DFIG is that it only requires a partial scale power converter rather than one rated for the full generator capacity. The DFIG is controlled by the rotor-side converter that operates at slip power. Hence, the rating of the converter required is lower than the rated output power. Several DFIGs on the order of 20 kW are used on the Mutriku oscillating wave column (OWC) plant [48]. However, the disadvantages of using DFIG in WECs include (1) a direct stator connection from DFIG to the grid, (2) the use of slip-ring assemblies in the rotor terminals that are severely degrading over time and require regular maintenance [49], and (3) low efficiency and control issues when operating below the rated speed [50]. Additionally, SCIGs and DFIGs exhibit limited adaptability to the highly variable and stochastic nature of wave energy conversion due to their optimal performance being constrained around rated speed operation. Their efficiency drops significantly when operating over a broad speed range, which is a key challenge in wave energy applications. Hence, traditional IGs and DFIGs are confined to PTO topologies that operate near the rated speed and are not the preferred machines for direct-drive PTOs that operate over a wide-speed range.

#### 3.1.2. Switched Reluctance Generators

Switched Reluctance Generators (SRGs) work on the principle of variable magnetic inductance. As shown in Figures 3b and 4b, SRGs consist of a salient pole rotor comprising a ferromagnetic material and stator slots for windings. A SRG generates electrical power as the rotor moves from a maximum-inductance configuration to a minimum-inductance one. The timing and phasing of current flow into the stator windings is decided by the power electronic converter based on the rotor position.

The merits of the SRG for WEC systems lie in its (1) simple structure; (2) cost-effectiveness; (3) absence of permanent magents (PMs), which eliminates challenges such as rare earth availability, demagnetization due to high-temperature operation, corrosion in the marine environment, etc. [51]; (4) high robustness; (5) broad speed range; and (6) possibility of DC power generation via current control, as proposed in [52].

The drawbacks of SRGs are as follows: (1) low power density and efficiency [53], (2) large torque ripple, and (3) high translator weight in the case of linear direct-drive

machines, and (4) high sensitivity to the phasing through which current is applied, which results in strict sensing and control requirements.

Researchers have been developing various advanced topologies to reduce the generator voltage ripple [54] and increase the power density [53] and torque density [55] to make SRG more suitable for WEC systems. However, obtaining optimal performance of SRG across various speed and load conditions corresponding to irregular waves is still challenging.

#### 3.1.3. Permanent Magnet Synchronous Generators

Traditional (rotary) PMSGs (Figure 3c,d) consist of PMs on the rotor and three-phase windings in the stator. PMSGs are considered surface-mounted if the magnets are positioned on the rotor surface, and interior magnet PMSGs if the magnets are embedded within the rotor. The magnitude and frequency of the Electro-motive Force (EMF) depend on the magnetic field's strength and the machine's speed.

A linear PMSG (Figure 4c,d) comprises a stator similar to that of a conventional rotary machine that has been unrolled and whose rotor is replaced by a translator [56].

The advantages of PMSGs for WECs include (1) high power density, (2) high efficiency, (3) broad speed operation range, (4) low weight and compact size, and (5) long lifetime.

The disadvantages of PMSG are (1) dependency on rare-earth magnets, (2) demagnetization of magnets at high temperatures, and (3) high initial cost.

### *3.2. Performance Comparison of EMG Topologies*

Having outlined the advantages and disadvantages of various generator types, we compare their suitability for WEC systems using figures of merit from the literature. These figures of merit include power density, which reflects the amount of power that can be generated relative to its weight. Efficiency measures how effectively the input mechanical energy is converted into electrical power, while the operating speed range indicates the generator's ability to adapt to fluctuating wave conditions. Torque ripple quantifies the periodic fluctuations in electromagnetic torque of EMG and has an influence on the dynamics of WECs. The power converter rating determines the cost and complexity of the system, with lower ratings generally being advantageous. Cost captures the overall economic feasibility of each topology, and reliability determines its long-term suitability for operation in marine environments. A qualitative comparison of different figures of merit for different topologies, based on data presented in the literature, is provided in Figure 5 [57,58], depicting a relative comparison of generator performance for wave energy applications.

The PMSG exhibits the highest power density owing to its high-flux permanent magnets and compact design. The SRG also benefits from a simple rotor structure but typically demonstrates lower magnetic flux utilization, limiting its torque per unit volume. The DFIG provides moderate power density, although the presence of slip ring assemblies and additional winding space reduces its compactness. When adapted for variable-speed operation with a full-scale converter, the SCIG becomes bulkier due to the absence of magnetic field control, resulting in relatively low power density across wide-speed applications.

With respect to efficiency, the PMSG maintains high values over a wide speed range due to low copper and core losses and strong magnetic coupling. The SRG, although magnet-free, can achieve good efficiency with optimized control but is prone to switching and iron losses caused by frequent excitation. The DFIG demonstrates good efficiency near synchronous speed but experiences significant losses under slip. The SCIG shows lower efficiency due to higher copper losses and the lack of active excitation control, making it less suitable for variable-speed operation.

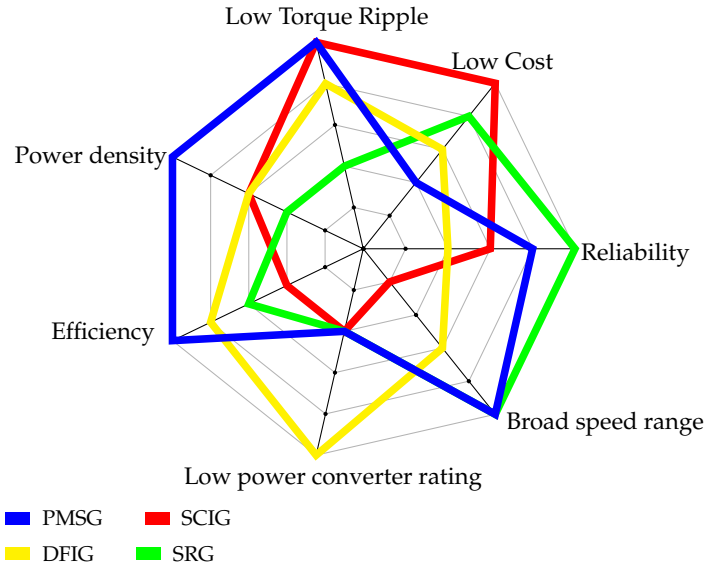


**Figure 5.** Performance comparison of generators for WEC systems.

In terms of power converters, the PMSG, SRG, and SCIG require full-scale converters for grid integration and variable-speed operation. The SRG additionally demands more complex control logic and may require a larger number of switches owing to its phase independence [59]. By contrast, the DFIG employs a partial-scale converter, which reduces both cost and conduction losses.

Regarding broad speed range capability, the PMSG effectively supports wide-speed operation through field weakening, maintaining torque control across the range. The SRG is inherently capable of ultra-wide speed ranges due to its reluctance-based torque generation and independent phase control. The DFIG allows operation within a moderate slip range, which may be insufficient for highly dynamic WEC profiles. The SCIG can achieve wide-speed operation with a full converter; however, its lack of torque control flexibility and lower efficiency at low speeds make it less optimal than machines specifically designed for variable-speed systems.

In terms of reliability, the PMSG performs well in wave energy applications due to its brushless design and elimination of slip rings, making it suitable for harsh ocean environments. Nevertheless, reliability may be affected by issues such as thermal demagnetization and permanent magnet corrosion. The SRG provides high reliability, featuring a completely passive rotor without windings or magnets, thus reducing the likelihood of component failure. The DFIG is less reliable in wave applications because its slip rings and brushes are prone to wear and require frequent maintenance. The SCIG, although mechanically simple and reliable in fixed-speed configurations, is less suitable for variable-speed operation due to increased thermal stress and lack of flux control.

To contextualize the preceding analysis, Table 1 provides an overview of recent wave energy generation projects, highlighting key aspects of the WEC device, PTO architecture, and generators used by each developer, as well as details of their recent known projects. While hydraulic PTOs played a pivotal role in early wave energy systems [60,61], recent developments are increasingly shifting towards a direct-drive paradigm. The energy conversion chain in direct-mechanical drive and direct-electric drive PTOs is similar to that of wind energy generation systems. Consequently, similar to the wind industry, the use of PMSG for wave energy has attracted significant interest both within the industry and in recent academic publications.

**Table 1.** WEC configuration of selected recent wave energy projects.

| Developer | WEC Device | PTO Type | Generator | Control Type (Power Flow) | Latest Project (Year) |
|---|---|---|---|---|---|
| Seabased [62] | Oscillating Body (Surface Point Absorber Buoy) | Direct Electric | Linear PMSG | Passive (Unidirectional) | Mauritius, Canary Islands (2023–ongoing) |
| CorPower Ocean [63,64] | Oscillating Body (Point Absorber) | Direct Mechanical | PMSG | Phase Control (Bidirectional) | HiWave-5, Portugal (2024) |
| AWS Ocean Energy [65] | Oscillating Body (Submerged Buoy) | Direct Electric | Linear Generator | Passive Control (Unidirectional) | EMEC Scapa Flow, Orkney (2022) |
| Eco Wave Power [66] | Oscillating Body (Shore-Mounted Oscillating Floaters) | Hydraulic | Rotary Generator | Hydraulic Damping (Unidirectional) | Portugal Project (2024–2026) |
| WavePiston [67,68] | Oscillating Body (Surface Point Absorber) | Hydraulic | Rotary Generator | Passive (Unidirectional) | PLOCAN, Gran Canaria (2024) |
| Carnegie Clean Energy [69] | Oscillating Body (Submerged Point Absorber) | Direct Mechanical | Rotary Generator | RL (Bidirectional) | CETO 6 Gen, Australia (2022) |
| Mocean Energy [70] | Oscillating Body (Hinged Raft Attenuator) | Direct Electric | Rotary PMSG | Adaptive Control (Bidirectional) | Blue Horizon (2025) |
| Oceantec Energías Mari-nas/IDOM [71] | Oscillating Water Column (OWC) | Pneumatic | Rotary Generator | Passive Control (Unidirectional) | EuropeWave Redeployment at BiMEP, Spain (2025) |
| Ocean Power Technologies [72] | Oscillating Body (Point Absorber) | Direct Mechanical | Rotary PMSG | Passive Control (Unidirectional) | PowerBuoy PB3 (2023) |
| AW-Energy (WaveRoller) [73] | Oscillating Wave Surge | Hydraulic | SCIG | Passive Control (Unidirectional) | ONDEP (2024) |

## 4. Permanent Magnet Synchronous Generator for Wave Energy Conversion Systems

With increasing attention to PMSGs for wave applications, this section reviews the design requirements and performance optimization strategies suited to the unique challenges of the wave environment. To highlight the specific demands of wave energy, a comparison with wind and tidal energy systems is presented, providing context for the differences in operational requirements. Key differences arise in input power characteristics, torque profiles, environmental exposure, thermal management, and control strategies. Table 2 summarizes these distinctions, emphasizing how PMSG operation and control behavior in wave applications differ fundamentally from those in wind and tidal systems.

The distinctive characteristics of WEC operation introduce several specific design challenges for PMSGs. Low and oscillatory rotational speeds, which often reverse direction within each wave cycle, intensify cogging torque due to interactions between permanent magnets and stator slots, leading to irregular startup behavior and reduced energy capture efficiency. Additionally, the highly variable and intermittent torque profiles characteristic of ocean waves cause frequent thermal cycling and prolonged operation at partial load, increasing the risk of magnet demagnetization and material fatigue compared with the more uniform low-speed drives used in wind or tidal systems.

**Table 2.** Key differences in PMSG requirements for WEC, wind, and tidal applications.

| Feature/Requirement | Wave Energy Systems | Wind Energy Systems | Tidal Energy Systems |
|---|---|---|---|
| Input power profile | Highly irregular, stochastic, high peak-to-average ratio [20,74,75] | Stochastic, mostly steady at a given wind speed with fluctuations due to turbulence [57,76] | Relatively steady and highly predictable tidal cycles with slow variation [77,78] |
| Power flow direction | Bidirectional (generator and motor modes in case of reactive control) [74,79,80] | Primarily unidirectional (generator mode) [57] | Unidirectional generation (occasional braking) [25,77] |
| Speed range | Very wide, extended near-zero-speed within each wave period [10,81] | Moderate, governed by rotor aerodynamics [57,76] | Narrow to moderate, governed by rotor hydrodynamics [25,78] |
| Torque characteristics | Always oscillatory, large torque reversals, frequent start and stop [82,83] | Steady at a given wind speed with fluctuations due to turbulence [57,84] | Smooth unidirectional torque, low reversal frequency [25,78] |
| Machine type prevalence | Rotary (geared) and linear PMSGs, magnetic gearing/tubular designs used [10,46,81,85] | Rotary PMSGs, geared or direct drive [57,76] | Rotary PMSGs dominant, often geared [25,77] |
| Environmental conditions | Partially or fully submerged depending on design, cyclic loads (high), corrosion protection and sealing of magnets/bearings if submerged, marine growth, array/wake effects (low to moderate) [20,86] | Onshore/offshore exposure, atmospheric corrosion, cyclic loads (low to moderate), array/wake effects in wind farms (moderate) [76] | Fully submerged, cyclic loads (moderate), corrosion protection and sealing of magnets and bearings, hydrostatic pressure, marine growth, array/wake effects (high) [77,78] |
| Thermal behavior | Frequent load cycling leads to thermal swings. Fully submerged designs benefit from seawater cooling; otherwise, air or internal liquid cooling is used [19,46] | Continuous rotation assists cooling [76] | Continuous rotation and steady tidal flow lead to smaller thermal swings, benefits from seawater cooling [25,78] |
| Control strategy demands | Fast transitions between motoring/generating, reactive control support [79,80,87] | MPPT-oriented speed/torque tracking [57,84] | MPPT-oriented control, fewer reversals [25,77] |

These operational demands indicate that conventional PMSG designs, originally developed for wind or tidal applications, may not fully satisfy the performance requirements of WECs. Consequently, advanced PMSG topologies have been developed specifically for WEC systems.

### *4.1. Advanced PMSG Topologies for WEC Systems*

The preceding analysis highlights that conventional PMSG configurations require specific adaptation to address the variable and oscillatory nature of WECs. This section therefore focuses on advanced design approaches that enhance performance in the marine environment.

#### 4.1.1. Construction

The construction is one of the crucial aspects of generator design in addressing low-speed challenges while optimizing efficiency. In addition to conventional rotary and linear generators, an advanced generator topology proposed for wave energy applications is the tubular linear generator [88]. This design features a cylindrical hollow stator that encloses a translator, equipped with a series of annular PMs arranged in alternating polarity.

The tubular structure offers simple construction, eliminates the need for end windings, and provides improved power density compared to traditional linear generators. Nevertheless, it requires a significant volume of PMs and a robust mechanical structure to secure the translator and maintain a fixed air gap. Furthermore, for WECs equipped with a submerged sealed generator, constructional features that facilitate effective heat dissipation are critical [89]. Materials with high thermal conductivity and protective coatings are often employed to mitigate thermal stress and magnet degradation [90,91] during prolonged operation at a partial load. These design modifications aim to enhance power density, efficiency, and compactness, thus improving the overall performance of PMSG.

#### 4.1.2. Magnetic Flux Orientation

The orientation of magnetic flux in PMSGs plays an important role in determining their efficiency, torque production, and suitability for direct-drive wave energy applications. Based on the direction of the magnetic flux across the air gap, PMSGs can be classified into three primary configurations: radial, axial, and transverse flux machines.

Radial flux machines are the most widely used configuration, where magnetic flux travels radially from the rotor to the stator. Although well established, these machines tend to exhibit reduced efficiency under low-speed, high-torque conditions. To address this limitation, the authors in [46] proposed the integration of magnetic gears with radial flux PMSGs, thereby improving performance through high-speed, low-torque input to the generator.

Axial flux machines feature a disc-shaped geometry, where the rotor lies between two stators and flux flows parallel to the shaft. This configuration enables high torque density and a compact footprint, making it particularly advantageous for low-speed, direct-drive systems [27,92]. Axial topologies also facilitate improved thermal management due to their larger surface area, which enhances heat dissipation and helps prevent demagnetization under cyclic thermal loading.

Transverse flux machines guide magnetic flux along a path perpendicular to both the axis of rotation and the direction of motion. These machines provide higher torque density compared to axial and radial machines but face challenges such as lower power factor and increased manufacturing complexity [93]. However, their modular structure can be beneficial in marine environments where ease of sealing and maintenance accessibility are important.

#### 4.1.3. Permanent Magnet Arrangement

The placement of PMs is crucial for optimizing magnetic flux linkage, which directly influences efficiency, torque density, and performance in PMSGs. Proper PM arrangement enhances the generator's ability to generate high torque at low speeds.

Conventional PMSGs typically mount PMs on the rotor or embed them within it, resulting in surface-mounted or interior magnet designs. These configurations are well established but face limitations in low-speed, high-torque applications, where they may experience reduced efficiency and increased losses.

The Halbach array is a specific PM arrangement where the magnets are oriented in a way that maximizes the magnetic flux on one side of the rotor while minimizing it on the opposite side. Figure 6a illustrates a simplified Halbach magnet arrangement, where the internal arrows indicate the magnetization direction, showing how the magnetic field is reinforced on one side and suppressed on the opposite side. This configuration enhances power and torque density by amplifying the magnetic field in one direction, which is particularly beneficial for applications requiring high torque density, such as direct drive wave energy converters. However, the Halbach array is susceptible to magnetic saturation under high load conditions, which can limit its performance [94,95].

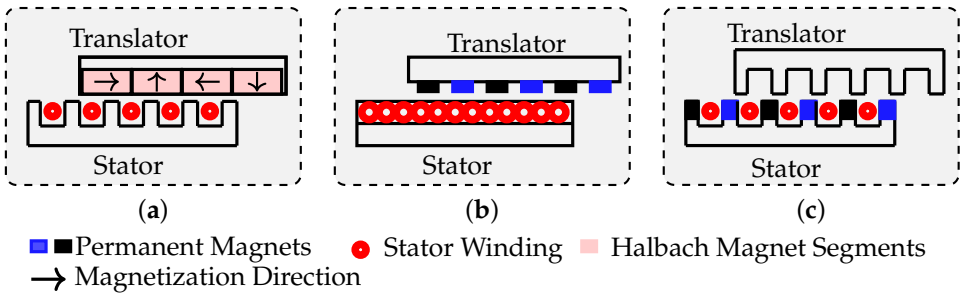


**Figure 6.** Structure of advanced linear generators. (**a**) Halbach PMSG; (**b**) Slotless PMSG; (**c**) Flux Switching PMSG.

#### 4.1.4. Stator Winding Arrangement

The configuration of the stator windings plays an important role in minimizing losses, reducing cogging torque, and improving cooling efficiency. These configurations can either be slotted or slotless, with variations such as fractional slot and minimal slot arrangements, each targeting specific performance enhancements.

Slotless machines (Figure 6b) have windings placed on the surface of the stator, and the absence of slots eliminates the attractive forces between the slots and PMs, thereby reducing cogging torque and torque ripple [96]. Nevertheless, this configuration offers limited winding space and lower cooling efficiency. However, its smoother magnetic field distribution contributes to a more sinusoidal EMF waveforms.

Fractional slot configurations maintain a fractional ratio of poles per phase to reduce cogging torque by minimizing the interaction between stator slots and rotor magnets. Although effective, these machines are more complex to manufacture and may experience increased winding resistance due to restricted conductor areas [97].

Minimal-slot configurations accommodate multiple winding turns within each slot, which helps reduce winding resistance; however, this approach also increases cogging torque because of higher magnetic saliency and stronger slot–pole interactions [98].

#### 4.1.5. Magnetic Topology

To enhance torque density and address challenges such as low-speed operation and high-torque requirements in wave energy systems, various magnetic topologies have been proposed for PMSGs. These topologies influence how the magnetic flux is generated, modulated, and directed within the generator, directly affecting its performance, particularly in low-speed, direct-drive applications. Several advanced magnetic topologies show promise in improving torque density and overall efficiency for wave energy conversion systems.

Vernier PMSGs, also known as magnetic gear-based machines, exploit magnetic field harmonics to achieve flux modulation between the rotor and stator. This mechanism enables high torque density at low speeds, making Vernier machines especially promising

for direct-drive wave energy converters. Several studies, including [99,100], demonstrate the effectiveness of Vernier topologies in achieving high power output and torque under oceanic conditions.

Flux-modulated PMSGs are closely related to Vernier machines but instead employ passive modulating structures, such as iron segments, to reshape the magnetic field. These machines also deliver enhanced torque density and have been explored for marine energy systems in conceptual and simulation-based studies [27].

Flux reversal PMSGs generates voltage by reversing the magnetic flux direction in the stator teeth as the rotor moves. Although less common in commercial deployment, this topology offers potential for compact direct-drive designs. Some experimental studies have proposed linear flux-reversal machines for wave energy capture, highlighting their efficient flux utilization and simple coil arrangements [101,102].

Flux-switching PMSGs (Figure 6c) differs from the above by relocating both permanent magnets and windings to the stator, while the rotor consists of passive laminated iron. As the rotor rotates, it periodically switches the magnetic flux paths between different stator teeth, dynamically modifying the magnetic circuit. This design enhances torque density and robustness while eliminating magnets or coils from moving parts. Although not yet widely adopted in commercial WECs, flux-switching machines have been extensively researched for their suitability in harsh marine environments [28,103–105].

Based on the analysis of the advantages and disadvantages of each design arrangement, it is clear that optimizing components such as permanent magnet positioning, stator winding configurations, and slot arrangements can significantly enhance the performance of a PMSG. These design aspects directly influence key performance metrics, including torque density, efficiency, and overall reliability. Quantitative details from representative studies, such as ranges of torque density, efficiency, and cogging torque, have been incorporated in Table 3, offering an overview of the respective advantages and challenges associated with each configuration.

**Table 3.** Compact design variations of PMSGs for wave energy systems.

| Ref. | Construction | PM Placement | Stator Winding | Advantages | Disadvantages |
|---|---|---|---|---|---|
| [96] | Tubular linear (slotless) | Surface-mounted | Distributed | 90% efficiency; cogging-free | Precise alignment; limited scalability |
| [106] | Tubular linear | Surface-mounted with auxiliary teeth | Distributed | 76% detent reduction | Precision fabrication; added complexity |
| [107] | Tubular linear | Halbach array | Concentrated | 82.6% detent reduction | Complex assembly; high rare-earth cost |
| [108] | Radial flux (magnetically geared) | Surface-mounted with gearing | Distributed | 82.8 kN·m/m$^3$ torque density; 90% efficiency | Large diameter; gear complexity |
| [46] | Radial flux (magnetically geared) | Surface-mounted with gearing | Distributed | >80 kN·m/m$^3$ torque density | Prototyping difficulty; thermal issues |
| [23] | Rotary IPM | Interior PM | Distributed | Efficiency 94–96.2% | Higher mass; material cost |
| [88] | Tubular linear (field modulated) | Surface-mounted with modulation poles | Concentrated | High thrust density (∼kN/m$^3$) | Complex design; tight tolerances |
| [99] | Linear vernier PMSG | Consequent-pole vernier | Concentrated | High thrust density (∼kN/kg) | High magnet demand; complex assembly |
| [100] | Dual-stator HTS linear vernier | Superconducting coils with vernier PMs | Concentrated | Very high thrust density (314 kN/m$^3$) | Cryogenic cost; reliability concerns |

## 5. Control Strategies for WEC Systems

The performance of a WEC depends not only on generator design but also on the effectiveness of its control strategy, which governs energy capture. Since each generator and PTO configuration exhibits distinct dynamic characteristics, the control approach must be tailored accordingly to ensure optimal performance under varying wave conditions. This section presents an overview of control strategies for WEC systems, focusing on modeling approaches, high-level control for energy maximization, and low-level control techniques that manage generator operation.

Figure 7 illustrates this energy conversion chain and its control structure. Depending on the system design, a DC-to-DC converter and energy storage system (ESS) may also be integrated to smooth power fluctuations and enhance grid compliance.

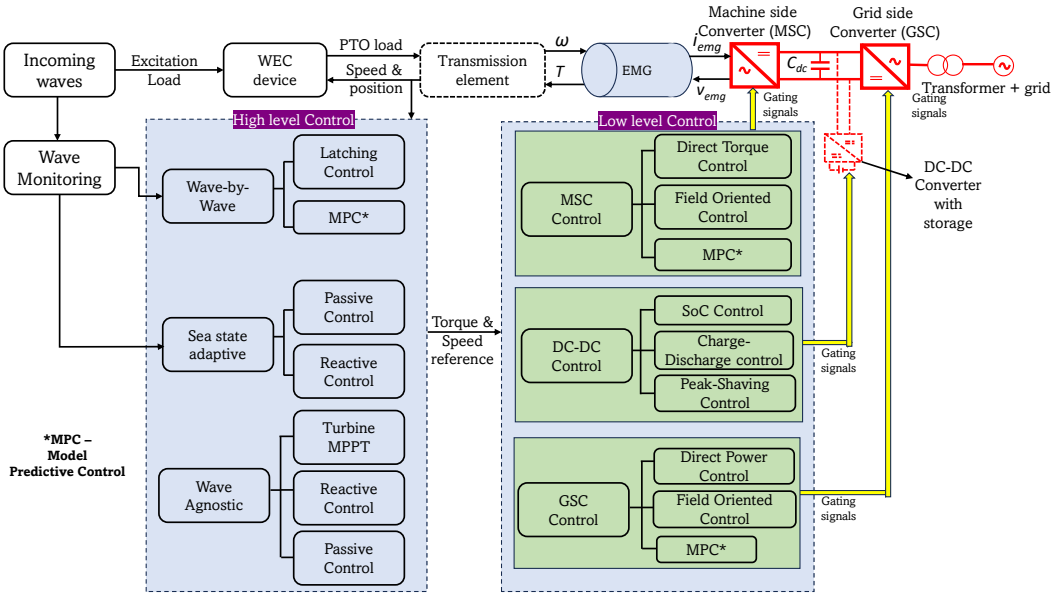


**Figure 7.** Diagram of a WEC power conversion chain, including its control.

To manage this multi-step conversion process, a hierarchical control strategy is employed. The high-level control aims to maximize energy absorption by adapting to changing sea state conditions and wave dynamics. It utilizes wave measurement data and feedback from the PTO system to generate reference signals, typically in the form of torque or force, for effective control of the PTO.

The low-level control implements these high-level commands across various subsystems, including the MSC, GSC, and the DC-to-DC converter. The DC to DC converter is essential for interfacing the ESS at the DC link, enabling charge and discharge operations. This helps maintain a constant or smoothed power output to the grid. The GSC maintains stable power flow and ensures grid compliance under varying ocean conditions [109]. While the GSC and ESS control strategies are similar to those used in other renewable energy systems, this work focuses on the MSC, which addresses the irregular dynamics unique to wave energy conversion.

To effectively design and evaluate such control strategies, it is essential to begin with a physically accurate yet computationally efficient model of the WEC. This model captures the hydrodynamic interaction with waves and the coupling with the PTO system, forming the foundation for both high-level and low-level control design.

### *5.1. Modeling of WEC Device*

The dynamic response of the WEC can be modeled using the generalized Cummins' equation [110,111] that describes the linear hydrodynamic behavior of a floating body, and accounts for the effects of added mass, radiation damping, hydrostatic restoring forces, and external excitations:

$$\mathbf{F}_{\text{wave}}(t) + \mathbf{F}_{\text{PTO}}(t) = (\mathbf{M} + \mathbf{A}_\infty)\ddot{\mathbf{q}}(t) + \int_0^t \mathbf{K}_{\text{rad}}(t-\tau)\,\dot{\mathbf{q}}(\tau)\,d\tau + \mathbf{K}_{\text{h}}\,\mathbf{q}(t) \tag{1}$$

where $\mathbf{q}(t) \in \mathbb{R}^n$ is a vector of generalized coordinates, representing the $n$ degrees of freedom of the WEC. Correspondingly, $\dot{\mathbf{q}}(t)$ and $\ddot{\mathbf{q}}(t)$ denote the velocity and acceleration vectors along these degrees of freedom. $\mathbf{M} \in \mathbb{R}^{n\times n}$ represents the inertia matrix of the WEC, while $\mathbf{A}_\infty \in \mathbb{R}^{n\times n}$ is the added-mass matrix at infinite frequency. The convolution kernel $\mathbf{K}_{\text{rad}}(t)$ accounts for radiation load. The term $\mathbf{K}_h \in \mathbb{R}^{n\times n}$ is the hydrostatic and gravitational stiffness matrix. $\mathbf{F}_{\text{PTO}}(t)$ denotes the force and torque vector from the power take-off system, while $\mathbf{F}_{\text{wave}}(t)$ is the generalized wave excitation force, which is a function of the incident wave frequency, and can be rendered as a superposition of harmonic contributions in the case of polychromatic irregular waves [111].

The instantaneous power extracted from the PTO is

$$P_{\text{PTO}}(t) = -\mathbf{F}_{\text{PTO}}(t)^\top \dot{\mathbf{q}}(t) \tag{2}$$

In order to extract maximum power from ocean waves over a target time window, the PTO system must apply an optimal control force to the WEC. Under the assumption of a linear dynamics, optimality conditions can be cast by resorting to a frequency domain formulation [112]. In the frequency domain, the radiation kernel $\mathbf{K}_{\text{rad}}$ reads as:

$$\hat{\mathbf{K}}_{\text{rad}}(\omega) = \hat{\mathbf{B}}_r(\omega) + j\omega\big(\hat{\mathbf{A}}_r(\omega) - \mathbf{A}_\infty\big) \tag{3}$$

where $\omega$ is the frequency coordinate, $\hat{\cdot}$ denotes the frequency domain equivalent of a time signal, $\hat{\mathbf{B}}_r(\omega)$ and $\hat{\mathbf{A}}_r(\omega)$ are frequency-dependent radiation damping and added mass matrices that account for the contribution of waves generated by the WEC motion.

Expressing the generalized PTO force in terms of a PTO impedance matrix $\mathbf{Z}_{\text{PTO}}(\omega)$, namely,

$$\hat{\mathbf{F}}_{\text{PTO}}(\omega) = -j\omega\mathbf{Z}_{\text{PTO}}(\omega)\hat{\mathbf{q}}(\omega). \tag{4}$$

a way to maximize the average extracted power is by resorting to impedance matching, i.e., rendering the PTO impedance equal to the complex conjugate of the WEC's mechanical impedance [113]:

$$\mathbf{Z}_{\text{PTO}}(\omega) = \mathbf{Z}^*_{\text{WEC}}(\omega), \text{ with } \mathbf{Z}_{\text{WEC}} = \hat{\mathbf{B}}_r(\omega) + j\left[\omega\big(\mathbf{M} + \hat{\mathbf{A}}_r(\omega)\big) - \frac{\mathbf{K}_{\text{h}}}{\omega}\right] \tag{5}$$

Equations (4) and (5) provide an ideal reference for the PTO load. In practical WEC applications, PTO systems are designed to act only upon a subset of the degrees of freedom. Moreover, due to physical limitations of the machinery and external constraints (moorings, end-stops, etc.), complex-conjugate control is seldom implemented, and sub-optimal strategies are used for PTO control.

### *5.2. High-Level Control Approaches*

High-level control strategies aim to maximize the absorbed wave energy by adjusting the PTO reference according to sea state and device dynamics. These methods rely on the system model presented earlier, where the wave excitation force drives the buoy dynamics and PTO interaction.

The generator control tracks the required PTO load reference set by the high-level controller for optimal WEC performance. As the controls of GSC and ESS do not differ substantially from those in other renewable applications, they will not be discussed in further detail here. Instead, more attention is paid to control aspects more specific to WECs, particularly the MSC.

The high-level control layer is responsible for determining the optimal reference to PTO subsystems to maximize energy extraction from ocean waves. Several types of high-level control can be envisaged, which rely on different degrees of knowledge of the incident waves and system dynamics. These control strategies involve tradeoffs in complexity, performance, and real-time implementation feasibility. Broadly, they can be categorized into three types: wave-by-wave control, sea-state adaptive control, and wave-agnostic control, as described below.

#### 5.2.1. Wave-by-Wave Control

Wave-by-wave control utilizes real-time wave measurements to create a set-point for the PTO force/torque. An example of wave-by-wave control is latching, which applies an ON–OFF force to the WEC device using a braking system. This control method prevents the device from moving during certain parts of the period, ensuring the optimal phase is achieved without reactive power flow in the machinery. However, the main challenge is determining when to latch and unlatch the WEC device's movement, particularly in irregular sea conditions [114].

Model predictive control (MPC) employs a discrete-time dynamic mode representation of WECs along with forecasts of the excitation force to maximize the power output within a given time frame (prediction horizon) [115]. MPC is utilized to identify the reference force/torque profiles that need to be generated by the generator. Wave-by-wave controls are virtually able to reach high power capture, but they typically require prior knowledge (e.g., prediction) of the incident waves.

#### 5.2.2. Sea State Adaptive Control

Sea state adaptive control optimizes energy capture based on wave height, period, and direction. Unlike real-time monitoring in wave-by-wave control, sea state adaptive control optimizes the PTO behavior based on broader time-averaged characteristics of the waves, such as peak period and significant wave height. Sea state adaptive control techniques typically encompass passive and reactive strategies to maximize wave energy extraction.

Passive (or resistive) control is one of the simplest and most robust strategies used in WEC systems. In this method, the load applied by the PTO is purely resistive (i.e., $\mathbf{Z}_{\mathrm{PTO}}(\omega)$ in (4) is real-valued), meaning that the reference torque or force is directly proportional to the velocity of the PTO. As the WEC moves in response to incoming waves, the control system applies a damping force that opposes this motion, thereby converting mechanical energy into electrical energy through the generator. The unidirectional power flow from the device to the power converter enables energy extraction, although maximum energy capture is not achieved, particularly under off-resonance conditions. Nevertheless, passive control offers advantages of simplicity, robustness, and ease of implementation.

Reactive control, in contrast, is intended to tune the WEC device with the wave by using reactive generator torques or forces, e.g., using a complex-valued PTO impedance, $\mathbf{Z}_{\mathrm{PTO}}(\omega)$. In this approach, the generator applies a reactive force to the WEC device that is proportional to its position or acceleration. This force is designed to bring the device into resonance, ensuring that the WEC speed is in phase with the wave excitation force. The process results in bidirectional power flow, with the generator operating as a motor during certain portions of the wave period.

#### 5.2.3. Wave-Agnostic Control

Wave-agnostic control means the use of pre-defined, optimized control logic established at the design stage without adapting the control to varying wave conditions. This control method does not explicitly use knowledge of wave parameters or wave elevation measurements, sacrificing power capture performance to pursue robust PTO operation [116]. An example in this category is the use of maximum power point tracking (MPPT) controls in pneumatic and hydraulic turbine PTOs in OWC or overtopping WECs, which aims to maximize the instantaneous PTO power output while neglecting the WEC's dynamics and global optimal performance [117].

The high-level control block produces torque or speed reference signals for the generator to follow, aiming to harness power from the waves under real wave conditions efficiently.

### *5.3. Low-Level Permanent Magnet Synchronous Generator Control Techniques*

The low-level control is responsible for executing the reference signals generated by the high-level controller. It directly manages the operation of key subsystems within the PTO to ensure stable and efficient power transfer. Specifically, the low-level control includes the control of the generator, the DC-to-DC converter, and the GSC. These components work together to regulate the PTO response, manage energy storage interactions, and maintain compliant power delivery to the grid under dynamic wave conditions. Within the low-level control framework, generator control is responsible for ensuring that the generator accurately follows the force/torque reference provided by the high-level controller. This section focuses on the modeling and control of PMSGs. The dynamic behavior of the PMSG is represented in a rotating reference frame using the $d-q-0$ transformation, which simplifies the control of torque and flux components. In this model, the space distribution of flux in the air gap produced by the permanent magnets is assumed to be sinusoidal, resulting in sinusoidal electromotive forces. The rotor magnet axis is taken to be aligned with the a-phase axis (Figure 8) when the rotor position is $\theta_{\mathrm{e}} = 0^{\circ}$. Furthermore, the influence of inductance saturation is disregarded.

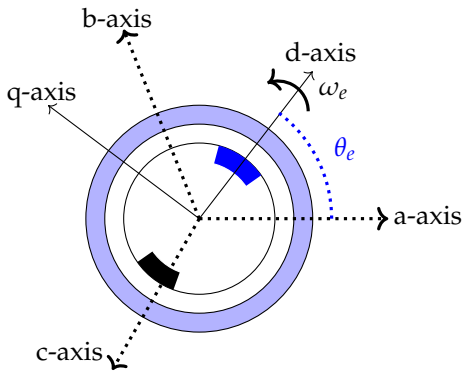


**Figure 8.** Winding and dq axis representation of PMSG, adapted from [118].

This section presents an overview of the modeling and control aspects of PMSGs, which relies on a model of the PMSG developed in a rotating reference frame whose dynamic voltage equations are given by

$$u_{\mathrm{sd}} = R_{\mathrm{s}} i_{\mathrm{sd}} + \frac{d\psi_{\mathrm{sd}}}{dt} - \omega_{\mathrm{e}} \psi_{\mathrm{sq}} \tag{6}$$

$$u_{\mathrm{sq}} = R_{\mathrm{s}} i_{\mathrm{sq}} + \frac{d\psi_{\mathrm{sq}}}{dt} + \omega_{\mathrm{e}} \psi_{\mathrm{sd}} \tag{7}$$

$$T_{\mathrm{e}} = \frac{3}{2} P(\psi_{\mathrm{sd}} i_{\mathrm{sq}} - \psi_{\mathrm{sq}} i_{\mathrm{sd}}) = \frac{3}{2} P(\psi_{\mathrm{m}} i_{\mathrm{sq}} - (L_{\mathrm{sd}} - L_{\mathrm{sq}}) i_{\mathrm{sd}} i_{\mathrm{sq}}) \tag{8}$$

where,

$$\psi_{\mathrm{sd}} = L_{\mathrm{sd}} i_{\mathrm{sd}} + \psi_{\mathrm{m}} \tag{9}$$

$$\psi_{\mathrm{sq}} = L_{\mathrm{sq}} i_{\mathrm{sq}} \tag{10}$$

$$P_{\mathrm{gen}} = \frac{3}{2}(u_{\mathrm{sd}} i_{\mathrm{sd}} + u_{\mathrm{sq}} i_{\mathrm{sq}}) \tag{11}$$

where $u_{\mathrm{sd}}$ and $u_{\mathrm{sq}}$ are the d and q axis voltages at the stator terminals; $i_{\mathrm{sd}}$ and $i_{\mathrm{sq}}$ are the d and q axis currents; $\psi_{\mathrm{sd}}$ and $\psi_{\mathrm{sq}}$ are the d and q axis flux components; $\omega_{\mathrm{e}}$ is the electrical speed; $R_{\mathrm{s}}$ is the stator resistance; $P$ is the number of pole pairs of the generator; $L_{\mathrm{sd}}$ and $L_{\mathrm{sq}}$ are the d and q-axis inductances, respectively; $\psi_{\mathrm{m}}$ is the permanent magnets' flux linkage; $P_{\mathrm{gen}}$ is the electrical power output of the generator, and $T_{\mathrm{e}}$ is the electro-mechanical torque output, that maps into a generalized PTO force acting on the WEC's degrees of freedom:

$$\mathbf{F}_{\mathrm{PTO}}(t) = T_e(t) \mathbf{H}_{\mathrm{PTO,g}}(t), \tag{12}$$

where $\mathbf{H}_{\mathrm{PTO,g}}$ is the Jacobian relating generator rotation to the WEC generalized coordinates (i.e., it transports the generator torque into generalized forces on the WEC degrees of freedom).

The equations above can be adapted for linear PMSGs, utilizing force and linear speed instead of torque and rotational speed [82,105]. When using rotary generators in direct mechanical drive PTOs, the force and speed of the PTO are related (usually a direct proportionality) to the torque and angular speed of the generator through the speed ratio of the mechanical transmission system. The rotating reference frame model of the PMSG serves as the foundation for implementing advanced control strategies to regulate torque and current under dynamic conditions. In wave energy applications, where low-speed operation and bidirectional power flow are common, accurate control is essential. The following sections present three widely used methods, field oriented control (FOC), direct torque control (DTC), and model predictive control (MPC), and their suitability for WEC systems. Table 4 presents the control adaptations required when applying these control techniques for advanced PMSG designs discussed in Section 4.1.

#### 5.3.1. Field-Oriented Control

FOC (Figure 9) is the predominant control strategy for PMSGs, including those employed in WEC systems. It is typically implemented as a cascaded control structure comprising an inner current- or torque-control loop and, when required, an outer speed-control loop. The inner loop regulates generator currents to track a reference torque set by the high-level controller. Accurate torque tracking in the inner loop depends on generating appropriate reference currents in the rotating *d-q* reference frame, which is a critical aspect of FOC performance.

**Table 4.** Control adaptation requirements for advanced PMSG topologies.

| Topology | Key Design Aspect | Control Adaptation Requirement |
| --- | --- | --- |
| Linear PMSG | Finite stroke, strong end effects, position-dependent EMF and inductance, detent force due to slotting [119] | End-of-stroke damping, position-dependent inductance/EMF compensation, detent-force or harmonic-current cancellation [120,121] |
| Tubular PMSG | Strong end effects [122] | End-effect compensation, observers enhanced for flux-position coupling, force ripple suppression, current-limit and thermal-aware control [123] |
| Axial-Flux PMSG | Disc geometry, high pole count, multi-disc stacking, potential non-uniform air gap [124] | Per-disc current balancing, cogging and torque-ripple minimization, temperature-dependent flux-weakening [125,126] |
| Transverse-Flux PMSG | 3D flux path, high leakage, strong harmonic content [127,128] | Extended dq or phase-coupled model, harmonic-rich EMF observers, leakage-aware flux estimation, predictive current control for ripple reduction [129] |
| Halbach-Array PMSG | Flux concentrated on one side, high air-gap flux density [130] | Early field-weakening, accurate EMF and flux estimation, strict demagnetisation-aware current limits, end-effect EMF spike compensation (for linear/tubular forms) [131] |
| Vernier PMSG | Magnetic gearing effect, very high effective pole count, significant space-time harmonics [132,133] | Electrical-angle scaling, harmonic current injection, high-bandwidth current control, mandatory high-resolution position sensing [134] |
| Flux-Modulated PMSG | Flux-modulating stator teeth, strong magnetic saturation, low power factor, high electrical frequency [135] | Modified dq model including modulation ratio, saturation-aware gain scheduling, torque-ripple minimization, preference for predictive/advanced current control [136] |
| Flux-Reversal PMSG | Flux reversal per pole, doubly salient topology, strong position-dependent inductance [137,138] | Flux-linkage map or online inductance estimation, torque ripple reduction, load-dependent flux observers, improved low-speed stability [139] |
| Flux-Switching PMSG | Inductance strongly dependent on rotor position [140,141] | Position-varying inductance compensation, predictive current control for ripple minimization, multi-layer dq coordination, limited sensorless capability [142,143] |

To achieve this, reference current generation techniques such as Field weakening (FW) and maximum torque per ampere (MTPA) are employed to determine the optimal $d$ and $q$ axis current components. These control blocks generate the current references based on the reference torque ($T_e^*$), set by the high-level control, and the sensed generator speed. The reference torque is constrained by the generator's maximum power rating at the corresponding operating speed. When operating below the base speed ($\omega_{base}$), MTPA aims to achieve maximum torque per stator current, thereby minimizing copper losses. For interior PMSGs, the optimal $d$ and $q$ axis stator current references can be calculated using Equations (15) and (16) [144].

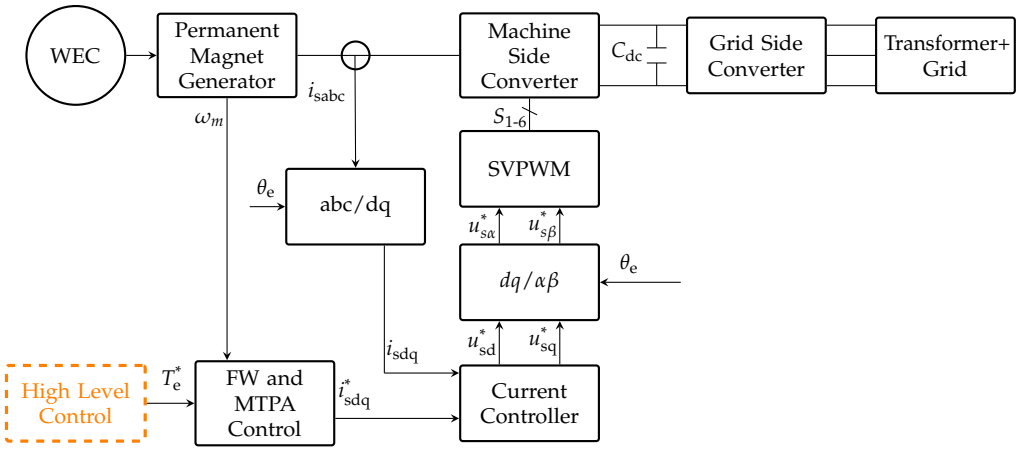


**Figure 9.** Field–Oriented Control of PMSG.

This approach becomes particularly important in salient pole machines, where both electromagnetic and reluctance torque components contribute significantly. The torque Equation (8) consists of two terms: the first represents electromagnetic torque, while the second captures reluctance torque. In the field-weakening (FW) region, where the magnetizing torque decreases, the reluctance torque supports continued torque generation, enabling performance beyond what non-salient machines can achieve.

Field weakening is essential when the generator operates above base speed to prevent overvoltage. It involves adjusting the demagnetizing $d$-axis current $i_{sd}$, which extends the speed range at the cost of reduced torque capability [79]. In surface-mounted PMSGs, where the $d$ and $q$ axis inductances are equal, FW is applied similarly by modulating $i_{sd}$ to meet voltage and current constraints defined by the generator and converter [145]. For such machines, MTPA is typically achieved by aligning the stator current along the $q$-axis up to base speed, with the corresponding optimal currents computed accordingly.

$$i^*_{sq} = \frac{T^*_e}{\frac{3}{2}P\psi_m} \tag{13}$$

$$i^*_{sd} = 0 \tag{14}$$

$$i^{*4}_{sq} + i^*_{sq}\frac{2T^*_e\psi_m}{3P(L_{sd}-L_{sq})^2} - \frac{4T^{*2}_e}{9P^2(L_{sd}-L_{sq})^2} = 0 \tag{15}$$

$$i^*_{sd} = -\frac{\psi_m}{2(L_{sd}-L_{sq})} - \sqrt{\left(\frac{\psi_m}{2(L_{sd}-L_{sq})}\right)^2 + (i^*_{sq})^2} \tag{16}$$

$$\omega_{base} = \frac{1}{P}\cdot\frac{U_{max}}{\sqrt{(L_{sq}i_{sq})^2 + (L_{sd}i_{sd}+\psi_m)^2}} \tag{17}$$

When the operating speed of the PMSG is beyond the base speed, it operates in the FW region while holding on to the voltage limit ($U_{max}$) of the generator/converter. The reference dq axis currents for the FW operation can be described using Equations (18) and (19).

$$\begin{aligned} &i^{*4}_{sq}\left(9P^2\omega^2_eL^2_{sq}(L_{sd}-L_{sq})^2\right) + i^{*2}_{sq}\left(9P^2\psi^2_mL^2_{sq}\omega^2_e - 9P^2(L_{sd}-L_{sq})^2U^2_{max}\right) \\ &- i_{sq}\left(12T^*_eP\psi_mL_{sd}L_{sq}\omega^2_e\right) + 4T^{*2}_eL^2_{sd}\omega^2_e = 0 \end{aligned} \tag{18}$$

$$i^*_{sd} = -\frac{\psi_m}{L_{sd}} + \frac{1}{L_{sd}}\sqrt{\left(\frac{U_{max}}{\omega_e}\right)^2 - L^2_{sq}i^{*2}_{sq}} \tag{19}$$

In the inner loop, the sensed currents from the generator are transformed into dq axis variables using the rotor angle measurement (estimation) from the position sensor (or indirectly calculated in the case of sensor-less control). In FOC, the current controllers generate reference voltages in the dq domain by comparing the sensed currents with reference currents and processing the error through corresponding controllers while incorporating appropriate feed-forward terms. Generally, the current controllers are of proportional-integral (PI) or proportional-integral-derivative (PID) type. These controllers minimize current errors in both the dq axes, thereby obtaining independent control of flux and torque in the machine, respectively. A key aspect of FOC involves tuning the inner control loops to be more responsive to input variations than the outer loop. This hierarchical design facilitates effective control. Eventually, space vector pulse width modulation (SVPWM) generates the corresponding gating signals based on sector selection corresponding to the required voltage at the generator's output.

Research has been carried out to modify the conventional FOC scheme to enhance the performance of WEC systems. The operation of PMSG is limited by the absolute voltage and current ratings determined by the converter connected to the MSC. In [13], the control operation is performed in three modes to optimize the maximum power extraction from WECs. In the first mode, the generator is operating within the rated conditions aiming at achieving MTPA condition. The second and third operation modes require field weakening. FW is further split into two modes. The second mode corresponds to the FW mode in which the machine operates beyond the base speed, and the optimal PTO torque/force reference dictated by the high-level control is physically realizable.

The third mode corresponds to the FW mode, in which the torque reference is not physically realizable. Consequently, the generator operates at its maximum rated torque, resulting in a reduced average power output from the WEC. To avoid this scenario, the implementation of high-level control strategies should be carried out, ensuring that the system accounts for the generator's intrinsic limitations in accurately producing force and torque references.

Ref. [146] considers the piecewise velocity method for the FOC implementation of a permanent magnet Synchronous Linear Generator (PMLG). In the piecewise velocity method, the generator accelerates at low speed under the action of mechanical load while not extracting any power, i.e., $i_{sd}, i_{sq} = 0$. Once the rotating speed of the generator reaches a defined threshold value, the conventional control techniques [147] of the generator take over.

FOC control operates at a fixed switching frequency and provides the advantages of low torque ripple and low computational burden. However, FOC provides a slow response to the perturbations of the system and typically requires rotor position data from the sensor.

In [79], a sensorless generator FOC is proposed, where the rotor position data is estimated from the generator voltage signals. The advantage of the sensorless control schemes is that they are cost-effective and improve the system's overall reliability as the sensor is prone to failures. The operation of these techniques near zero speed still needs to be well-established, as the sensorless techniques rely on the induced EMF in the generator in some form to calculate the rotor position.

#### 5.3.2. Direct Torque Control

DTC (Figure 10) is also one of the popular control strategies for PMSG applications. The DTC estimates the torque and flux of the machine at an operating point by using the measured current and Equations (8)–(10). The estimated torque and flux values are then compared to the corresponding reference values determined based on the wave condition,

and hysteresis controllers are then used to determine the sector selection when SVPWM technique is utilized. DTC provides a fast dynamic response to torque fluctuations but operates at variable switching frequency. However, the implementation of switching-table-based DTC also provides benefits similar to FOC's by switching at a constant frequency.

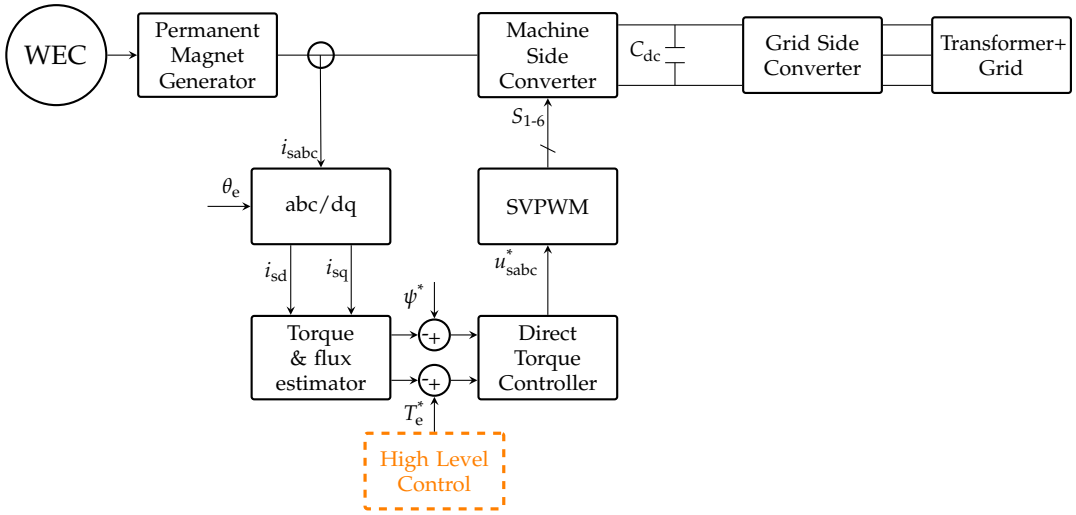


**Figure 10.** Direct–Torque Control of PMSG.

The wave energy converter developed for [148] utilizes a combination of DTC for PMSG and direct power control (DPC) for GSC control to obtain low distortion of the current injected into the grid. As the performance of the conventional DTC is based on a switching table, the torque ripple is high if the sampling frequency is low, although it offers a fast and robust control compared to FOC.

While DTC offers fast torque response and simplified implementation, its inherent torque ripple and variable switching frequency can pose challenges in wave energy systems that require smooth and efficient operation. Table 5 presents a comparative analysis of DTC and FOC, outlining their respective advantages, limitations, and implementation requirements. This comparison helps inform the control strategy selection based on the performance and reliability criteria specific to WEC applications.

**Table 5.** Comparison of FOC and DTC for generator control in WECs.

| Feature | Field-Oriented Control (FOC) | Direct Torque Control (DTC) |
|---|---|---|
| Efficiency | High across wide speed range | May vary due to switching losses |
| Wide speed range | Stable control | Uses voltage vector control |
| Low-speed operation | Precise | Needs advanced methods |
| Rotor position required | Yes | No |
| Sensed variables | Currents, voltages, rotor position | Currents and voltages |
| Estimated variables | Rotor flux position | Torque and stator flux |
| Torque response | Slower | Faster |
| Switching frequency | Constant | Variable |
| Steady-state behavior | Low ripple (torque/flux) | Higher ripple/distortion |
| Parameter sensitivity | $L_{sd}$, $L_{sq}$, $\psi_m$ | Mainly stator resistance |
| Control complexity | Moderate (transformations) | Simple (no transformations) |

#### 5.3.3. Low-Level Model Predictive Control

MPC (Figure 11) applied to electrical machines and power electronics uses a model of the system to provide future forecasts [149]. The sensed generator voltages and currents

are used to obtain the present system states, which include key dynamic variables such as rotor flux linkage, rotor position, and angular velocity. The cost function considers the variation of reference values compared to the predicted ones [150] along with the constraints corresponding to the maximum generator/converter voltage and current and the maximum allowable force and velocity of the WEC device. The optimal stator voltage vector is selected based on the cost function minimization. The performance of MPC depends, among other things, on the number of voltage vectors utilized to represent each segment of the space vector modulation. For instance, a classical MPC that uses a single optimal stator voltage vector for each switching cycle is similar to that of the selection-table-based DTC. Hence, a single optimal voltage vector-based MPC leads to variable switching frequency and increased torque ripple as compared to FOC and voltage modulator-based DTC discussed in Section 5.3.2. Two-vector MPC uses an optimal and zero vector and has a lower torque ripple than classical MPC [151].

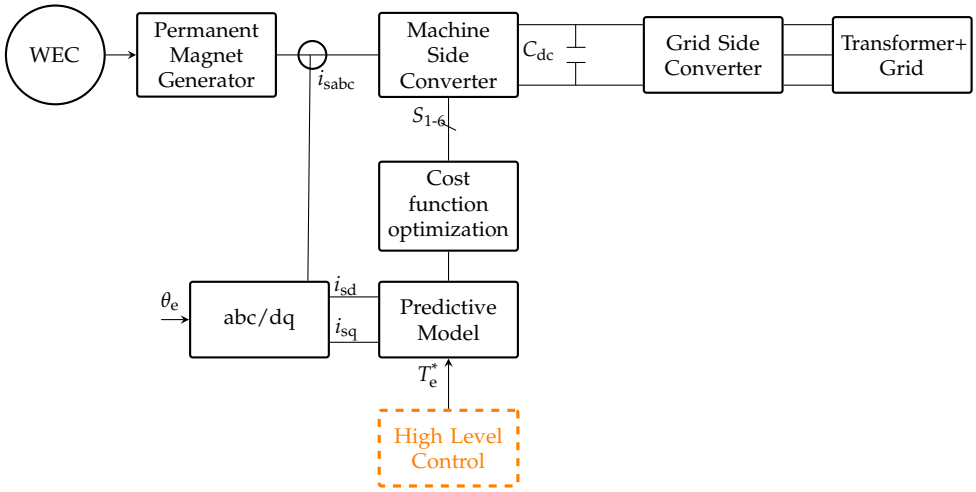


**Figure 11.** MPC (low–level) of PMSG.

In the article [152], a model predictive direct current control is proposed in which four vectors are applied, out of which two active and two zero vectors in each switching cycle, thus offering a fast and robust torque control to deal with wave variations. The results of the article indicate that the proposed control scheme provides a fixed switching frequency with limited torque ripple and is easy to implement.

### *5.4. Fault-Tolerant Control*

PMSGs used in direct drive PTOs are particularly susceptible to a range of electrical and mechanical faults, including open-switch and open-leg faults in converters, inter-turn short circuits, partial demagnetization, and sensor failures in current, speed, or position measurements [153]. Ensuring continuous energy conversion performance under these conditions requires advanced fault detection and fault-tolerant control (FTC) strategies integrated within the high-level control framework of the WEC.

Several studies have explored WEC-specific FTC methodologies. Ref. [154] presents a fault diagnosis and compensator scheme that detects sensor and actuator faults in real time and applies an optimal control strategy to maintain torque and maximize energy capture under stochastic wave excitation. Hardware-in-the-loop investigations [155] demonstrate that WEC controllers can tolerate sensor, actuator, and model mismatch faults, validating the application of FTC strategies to real-time PTO drives. Reviews of condition monitoring

and FTC techniques [153,156] provide a comprehensive overview of existing methods and highlight the importance of ensuring PTO reliability in the variable marine environment.

Specific implementations of WEC-targeted FTCs include damping injection-based control [157], which maintains torque and system stability under fault conditions, and robust control strategies designed for floating oscillating water column WECs [158], which ensure continued operation despite open-switch faults in converters. These approaches illustrate the capability of high-level control strategies to accommodate electrical and mechanical disturbances while sustaining energy conversion performance.

The advantages of integrating FTC within WEC control systems include the ability to maintain energy capture under partial failures, reduce downtime, and avoid costly offshore interventions. Approaches such as multiphase machine topologies, fault-resilient vector control, and model-predictive control provide inherent redundancy and adaptability, enhancing the reliability and availability of PTO systems [153,155]. Limitations remain in terms of increased controller complexity, dependence on accurate system modeling, and the requirement for extensive validation under realistic wave conditions.

Incorporating FTC into the high-level WEC control framework is essential for ensuring robust operation. By combining fault detection, reconfigurable control strategies, and WEC-specific adaptations, these methods allow for reliable energy conversion even under faulty conditions.

## 6. Conclusions

This paper presented a review of advanced PMSG topologies and control strategies for WEC systems. Various PMSG configurations, including tubular designs, Halbach arrays, axial and transverse flux machines, were evaluated based on their potential to address the challenges associated with low-speed, high-torque, and highly dynamic wave environments. These topologies offer improvements in power density, low-speed performance, and overall efficiency, making them strong candidates for direct-drive WEC applications. In addition, the paper highlighted the critical role of generator control strategies in maintaining performance under variable and unpredictable sea conditions. The integration of optimized generator designs with advanced control schemes is essential to enhancing the efficiency, robustness, and cost-effectiveness of WEC systems.

Future research should focus on the development of modular generator architectures to improve scalability, fault tolerance, and ease of maintenance in WEC deployments. Permanent magnet-assisted reluctance machines also present a promising alternative, offering high torque density and reduced dependency on rare-earth materials. However, the application of these systems in wave energy is currently challenged by issues such as torque ripple, control complexity under bidirectional motion, magnet retention concerns, and thermal management. To address these challenges, the development of advanced machine configurations and topologies is essential. On the control side, while advanced design options for wave energy generators have been explored, there is relatively limited literature addressing the specific control challenges associated with these advanced topologies and strategies for effectively handling them under stochastic and bidirectional wave conditions. The development of robust and adaptive algorithms capable of responding to these conditions remains a critical area for improvement. These advances will play a key role in enhancing energy capture efficiency and ensuring the reliable operation of wave energy systems in real-world environments, ultimately facilitating the commercialization of wave energy.

**Author Contributions:** Conceptualization, B.M., G.M. and E.T.; formal analysis, B.M. and G.M.; writing—original draft preparation, B.M.; writing—review and editing, B.M., G.M. and E.T.; visualization, B.M.; supervision, E.T. All authors have read and agreed to the published version of the manuscript.

**Funding:** The work is carried out as a part of the "Blue for Green" project funded by the 5x1000 2021 fundraising campaign of the University of Trento (with the support of Dolomiti Energia) in cooperation with the strategic area Oceans of NTNU.

**Data Availability Statement:** Not applicable.

**Conflicts of Interest:** The authors declare no conflicts of interest.

## Abbreviations

The following abbreviations are used in this manuscript:

| | |
|---|---|
| DPC | Direct power control |
| DTC | Direct torque control |
| DFIG | Doubly-fed induction generator |
| EMF | Electro-motive Force |
| EMG | Electro-magnetic generator |
| ESS | Energy storage system |
| FOC | Field oriented control |
| FW | Field weakening |
| GSC | Grid side converter |
| HTS | High temperature superconductor |
| IG | Induction generator |
| MPC | Model predictive control |
| MPDCC | Model predictive direct current control |
| MPPT | Maximum power point tracking |
| MSC | Machine side converter |
| MTPA | Maximum torque per ampere |
| OPT | Ocean Power Technologies |
| ORPC | Ocean Renewable Power Company |
| OWC | Oscillating wave column |
| PI | Proportional-integral |
| PID | Proportional-integral-derivative |
| PM | Permanent magnet |
| PMLG | Permanent magnet synchronous linear generator |
| PMSG | Permanent Magnet Synchronous Generator |
| PTO | Power take-off |
| PWM | Pulse width modulation |
| SCIG | Squirrel cage induction generator |
| SPWM | Sinusoidal pulse width modulation |
| SRG | Switched Reluctance Generator |
| SVM | Space vector modulation |
| SVPWM | Space vector pulse width modulation |
| VSC | Voltage source converter |
| WEC | Wave energy converter |

## References


1. Wave Energy Converter Market Projected to Expand at a CAGR of 4.26% from 2023 to 2030, Data by Contrive Datum Insights. 2023. Available online: https://www.globenewswire.com/news-release/2023/07/18/2706379/32656/en/Wave-and-Tidal-Energy-Market-to-Grow-at-a-CAGR-of-23-5-from-2022-to-2031-Reaching-USD-40-8-Billion-As-per-TMR-Study.html#:~:text=%2D%20The%20global%20wave%20and%20tidal,23.5%25%20between%202022%20and%202031 (accessed on 13 May 2025).
2. Mueller, M.A.; Polinder, H.; Baker, N. Current and Novel Electrical Generator Technology for Wave Energy Converters. In Proceedings of the 2007 IEEE International Electric Machines & Drives Conference, Antalya, Turkey, 3–5 May 2007; Volume 2, pp. 1401–1406. [CrossRef]
3. Li, H.; Shi, X.; Kong, W.; Kong, L.; Hu, Y.; Wu, X.; Pan, H.; Zhang, Z.; Pan, Y.; Yan, J. Advanced wave energy conversion technologies for sustainable and smart sea: A comprehensive review. *Renew. Energy* **2025**, *238*, 121980. [CrossRef]
4. Ulum Arga Pratama Zakaria, M.F.; Mukhtasor. State of the art of Power Take Off (PTO) systems in Wave Energy Converter (WEC). *Ocean. Eng.* **2025**, *335*, 121669. [CrossRef]
5. Têtu, A. Power Take-Off Systems for WECs. In *Handbook of Ocean Wave Energy*; Pecher, A., Kofoed, J.P., Eds.; Springer International Publishing: Cham, Switzerland, 2017; pp. 203–220. [CrossRef]
6. Tom, N. Review of Wave Energy Converter Power Take-Off Systems, Testing Practices, and Evaluation Metrics. In Proceedings of the ASME International Mechanical Engineering Congress and Exposition, IMECE 2022, Columbus, OH, USA, 30 October–3 November 2022; Volume 6, p. V006T08A065. [CrossRef]
7. Faiz, J.; Nematsaberi, A. Linear electrical generator topologies for direct-drive marine wave energy conversion—An overview. *IET Renew. Power Gener.* **2017**, *11*, 1163–1176. [CrossRef]
8. Zhang, Z.; Wu, B.; Lu, Q.; Xu, W. Novel Linear Generator Concepts and Topologies for Wave Energy Conversion Systems: A Review. In Proceedings of the 2021 13th International Symposium on Linear Drives for Industry Applications (LDIA), Wuhan, China, 1–3 July 2021; pp. 1–6. [CrossRef]
9. Polinder, H.; Mecrow, B.; Jack, A.; Dickinson, P.; Mueller, M. Conventional and TFPM linear generators for direct-drive wave energy conversion. *IEEE Trans. Energy Convers.* **2005**, *20*, 260–267. [CrossRef]
10. Polinder, H.; Damen, M.; Gardner, F. Linear PM Generator system for wave energy conversion in the AWS. *IEEE Trans. Energy Convers.* **2004**, *19*, 583–589. [CrossRef]
11. Coe, R.G.; Bacelli, G.; Forbush, D. A practical approach to wave energy modeling and control. *Renew. Sustain. Energy Rev.* **2021**, *142*, 110791. [CrossRef]
12. Shek, J.; Macpherson, D.; Mueller, M. Phase and Amplitude Control of a Linear Generator for Wave Energy Conversion. In Proceedings of the 2008 4th IET Conference on Power Electronics, Machines and Drives, York, UK, 2–4 April 2008; pp. 66–70. [CrossRef]
13. Oh, Y.J.; Park, J.S.; Hyon, B.J.; Lee, J. Novel Control Strategy of Wave Energy Converter Using Linear Permanent Magnet Synchronous Generator. *IEEE Trans. Appl. Supercond.* **2018**, *28*, 5204705. [CrossRef]
14. Amon, E.A.; Brekken, T.K.A.; Schacher, A.A. Maximum Power Point Tracking for Ocean Wave Energy Conversion. *IEEE Trans. Ind. Appl.* **2012**, *48*, 1079–1086. [CrossRef]
15. Sousounis, M.C.; Shek, J. Wave-to-Wire Power Maximization Control for All-Electric Wave Energy Converters with Non-Ideal Power Take-Off. *Energies* **2019**, *12*, 2948. [CrossRef]
16. Ringwood, J.V.; Zhan, S.; Faedo, N. Empowering wave energy with control technology: Possibilities and pitfalls. *Annu. Rev. Control* **2023**, *55*, 18–44. [CrossRef]
17. Said, H.A.; Ringwood, J.V. Grid integration aspects of wave energy—Overview and perspectives. *IET Renew. Power Gener.* **2021**, *15*, 3045–3064. [CrossRef]
18. Zhang, J.; Yu, H.; Chen, M. Direct-Drive wave energy conversion with linear generator: A review of research status and challenges. *IET Renew. Power Gener.* **2023**, *17*, 1020–1034. [CrossRef]
19. Mueller, M.A.; Burchell, J.; Chong, Y.C.; Keysan, O.; McDonald, A.; Galbraith, M.; Subiabre, E.J.P.E. Improving the Thermal Performance of Rotary and Linear Air-Cored Permanent Magnet Machines for Direct Drive Wind and Wave Energy Applications. *IEEE Trans. Energy Convers.* **2019**, *34*, 773–781. [CrossRef]
20. de O. Falcão, A.F. Wave energy utilization: A review of the technologies. *Renew. Sustain. Energy Rev.* **2010**, *14*, 899–918. [CrossRef]
21. Penalba, M.; Ringwood, J.V. A Review of Wave-to-Wire Models for Wave Energy Converters. *Energies* **2016**, *9*, 506. [CrossRef]
22. Morimoto, S.; Sanada, M.; Takeda, Y. Wide-speed operation of interior permanent magnet synchronous motors with high-performance current regulator. *IEEE Trans. Ind. Appl.* **1994**, *30*, 920–926. [CrossRef]
23. Rahman, A.; Farrok, O.; Islam, M.R.; Xu, W. Recent Progress in Electrical Generators for Oceanic Wave Energy Conversion. *IEEE Access* **2020**, *8*, 138595–138615. [CrossRef]

24. Bhende, C.N.; Mishra, S.; Malla, S.G. Permanent Magnet Synchronous Generator-Based Standalone Wind Energy Supply System. *IEEE Trans. Sustain. Energy* **2011**, *2*, 361–373. [CrossRef]
25. Benelghali, S.; Benbouzid, M.E.H.; Charpentier, J.F. Comparison of PMSG and DFIG for marine current turbine applications. In Proceedings of the XIX International Conference on Electrical Machines—ICEM 2010, Rome, Italy, 6–8 September 2010; IEEE: Piscataway, NJ, USA, 2010; pp. 1–6. [CrossRef]
26. Tokat, P.; Thiringer, T. Comparison of Interior, V-Shaped, Surface Mounted Permanent Magnet and Permanent Magnet Assisted Synchronous Reluctance Generators Used as a Wave Energy Converter Generator. In Proceedings of the 2018 XIII International Conference on Electrical Machines (ICEM), Alexandroupoli, Greece, 3–6 September 2018; pp. 1419–1425. [CrossRef]
27. Huang, L.; Li, Y.; Wei, L.; Chen, M. Comparison Research on Axial Flux Modulation Generators for Linear-rotary Wave Energy Conversion. In Proceedings of the 2022 IEEE 20th Biennial Conference on Electromagnetic Field Computation (CEFC), Denver, CO, USA, 24–26 October 2022; pp. 1–2. [CrossRef]
28. Fernando, N.; Nutkani, I.U.; Saha, S.; Niakinezhad, M. Flux switching machines: A review on design and applications. In Proceedings of the 2017 20th International Conference on Electrical Machines and Systems (ICEMS), Sydney, Australia, 11–14 August 2017; pp. 1–6. [CrossRef]
29. Torre-Enciso, Y.; Ortubia, I.; López de Aguileta, L.I.; Marqués, J. Mutriku Wave Power Plant: From the Thinking Out to the Reality. In Proceedings of the International Conference on Ocean Energy, Honolulu, HI, USA, 31 May–5 June 2009. Available online: https://api.semanticscholar.org/CorpusID:195835884 (accessed on 13 May 2025).
30. The Hawaii Wave Surge Energy Converter (HAWSEC). 2022. Available online: https://www.offshore-energy.biz/hawsec-wave-energy-device-undergoes-sea-trials-in-hawaii/ (accessed on 13 May 2025).
31. Whittaker, T.; Collier, D.; Folley, M.; Osterried, M.; Henry, A.; Crowley, M. The Development of Oyster—A Shallow Water Surging Wave Energy Converter. In Proceedings of the 7th European Wave and Tidal Energy Conference (EWTEC 2007), Porto, Portugal, 11–13 September 2007; p. 6.
32. Suwanapingkarl, P.; Srivallop, K. Reviews Existing Technologies and Proposes 'E8-PowerBuoys' Nano-Scale Generator of Tidal And Wave Energy For River And Ocean. In Proceedings of the 2020 International Conference on Power, Energy and Innovations (ICPEI), Chiang Mai, Thailand, 14–16 October 2020; pp. 85–88. [CrossRef]
33. Polinder, H.; Scuotto, M. Wave energy converters and their impact on power systems. In Proceedings of the 2005 International Conference on Future Power Systems, Amsterdam, The Netherlands, 16–18 November 2005; p. 9. [CrossRef]
34. Rubino, L.; Contestabile, P.; Langella, R.; Vicinanza, D. Dynamic Model of the Seawater Low-Head Turbine for Wave Energy Conversion. In Proceedings of the 2023 International Conference on Clean Electrical Power (ICCEP), Terrasini, Italy, 27–29 June 2023; pp. 303–308. [CrossRef]
35. Moretti, G.; Fontana, M.; Vertechy, R. Modeling of a Heaving Buoy Wave Energy Converter with Stacked Dielectric Elastomer Generator. In Proceedings of the ASME 2014 Conference on Smart Materials, Adaptive Structures and Intelligent Systems, Newport, RI, USA, 8–10 September 2014; Volume 1, p. V001T03A020. [CrossRef]
36. Bombora Wave Power—mWave Technology Overview. 2023. Available online: https://bomborawave.com/mwave/ (accessed on 13 May 2025).
37. Anaconda. 2023. Available online: https://energy.soton.ac.uk/anaconda-wave-energy-converter-concept/ (accessed on 13 May 2025).
38. Engin, C.D.; Yeşildirek, A. Designing and modeling of a point absorber wave energy converter with hydraulic power take-off unit. In Proceedings of the 2015 4th International Conference on Electric Power and Energy Conversion Systems (EPECS), Sharjah, UK, 24–26 November 2015; pp. 1–6. [CrossRef]
39. Kim, S.J.; Koo, W. Numerical Study on a Multibuoy-Type Wave Energy Converter with Hydraulic PTO System Under Real Sea Conditions. *IEEE J. Ocean. Eng.* **2021**, *46*, 573–582. [CrossRef]
40. Liermann, M.; Samhoury, O.; Atshan, S. Energy efficiency of pneumatic power take-off for wave energy converter. *Int. J. Mar. Energy* **2016**, *13*, 62–79. [CrossRef]
41. Yao, Z.; Wan, Z.; Wang, J.; Chao, D.; Ji, H.; Zhang, D. The structure design and hydrodynamic study of the multi-level overtopping wave power device. In Proceedings of the OCEANS 2017—Aberdeen, Aberdeen, UK, 19–22 June 2017; pp. 1–5. [CrossRef]
42. Liang, C.; Ai, J.; Zuo, L. Design, fabrication, simulation and testing of an ocean wave energy converter with mechanical motion rectifier. *Ocean. Eng.* **2017**, *136*, 190–200. [CrossRef]
43. Li, X.; Liang, C.; Chen, C.A.; Xiong, Q.; Parker, R.G.; Zuo, L. Optimum power analysis of a self-reactive wave energy point absorber with mechanically-driven power take-offs. *Energy* **2020**, *195*, 116927. [CrossRef]
44. Chen, C.A.; Li, X.; Zuo, L.; Ngo, K.D.T. Circuit Modeling of the Mechanical-Motion Rectifier for Electrical Simulation of Ocean Wave Power Takeoff. *IEEE Trans. Ind. Electron.* **2021**, *68*, 3262–3272. [CrossRef]

45. Moretti, G.; Santos Herran, M.; Forehand, D.; Alves, M.; Jeffrey, H.; Vertechy, R.; Fontana, M. Advances in the development of dielectric elastomer generators for wave energy conversion. *Renew. Sustain. Energy Rev.* **2020**, *117*, 109430. [CrossRef]
46. Johnson, M.; Polinder, H.; Mueller, M.; Tavner, P.; McDonald, A. Design and performance of a magnetically geared generator for wave energy applications. In Proceedings of the 2017 IEEE Energy Conversion Congress and Exposition (ECCE), Cincinnati, OH, USA, 1–5 October 2017; pp. 1–8. [CrossRef]
47. Baninajar, H.; Modaresahmadi, S.; Wong, H.Y.; Bird, J.Z.; Williams, W.; DeChant, B.; Southwick, P. A Dual-Stack Coaxial Magnetic Gear for a Wave Energy Conversion Generator. *IEEE Trans. Magn.* **2022**, *58*, 8003012. [CrossRef]
48. M'zoughi, F.; Garrido, I.; Bouallègue, S.; Ayadi, M.; Garrido, A. Intelligent Airflow Controls for a Stalling-Free Operation of an OscillatingWater Column-Based Wave Power Generation Plant. *Electronics* **2019**, *8*, 70. [CrossRef]
49. Nallagowden, P.; Varma, R.; Memonn, A.H. Performance improvement of synchronous permanent magnet generator for oscillating water column (OWC) wave energy converter. In Proceedings of the 2016 IEEE International Conference on Power and Energy (PECon), Melaka, Malaysia, 28–29 November 2016; pp. 792–796. [CrossRef]
50. Hazra, S.; Dean, A.G.; Bhattacharya, S. Doubly-fed induction generator enabled power generation in ocean wave energy conversion system. In Proceedings of the 2015 IEEE Energy Conversion Congress and Exposition (ECCE), Montreal, QC, Canada, 20–24 September 2015; pp. 6978–6985. [CrossRef]
51. Sun, Z.G.; Cheung, N.C.; Zhao, S.W.; Lu, Y.; Shi, Z.H. Design and simulation of a linear Switched Reluctance Generator for wave energy conversion. In Proceedings of the 2011 4th International Conference on Power Electronics Systems and Applications, Hong Kong, China, 8–10 June 2011; pp. 1–5. [CrossRef]
52. Luo, H.; Chen, K.; Pan, J. Comparative Study of Voltage Control for Linear Switched Reluctance Generator for Wave Generation System. In Proceedings of the 2020 8th International Conference on Power Electronics Systems and Applications (PESA), Hong Kong, China, 7–10 December 2020; pp. 1–5. [CrossRef]
53. Wang, D.; Shao, C.; Wang, X.; Zhang, C. Performance Characteristics and Preliminary Analysis of Low Cost Tubular Linear Switch Reluctance Generator for Direct Drive WEC. *IEEE Trans. Appl. Supercond.* **2016**, *26*, 0612205. [CrossRef]
54. Pan, J.F.; Zou, Y.; Cheung, N.; Cao, G.Z. On the Voltage Ripple Reduction Control of the Linear Switched Reluctance Generator for Wave Energy Utilization. *IEEE Trans. Power Electron.* **2014**, *29*, 5298–5307. [CrossRef]
55. Du, J.; Liang, D.; Liu, X. Performance Analysis of a Mutually Coupled Linear Switched Reluctance Machine for Direct-Drive Wave Energy Conversions. *IEEE Trans. Magn.* **2017**, *53*, 8108110. [CrossRef]
56. Qiu, S.; Zhao, W.; Zhang, C.; Shek, J.K.H.; Wang, H. A Novel Structure of Tubular Staggered Transverse-Flux Permanent-Magnet Linear Generator for Wave Energy Conversion. *IEEE Trans. Energy Convers.* **2022**, *37*, 24–35. [CrossRef]
57. Chen, W.; Zheng, T.; Yang, D.; Zhang, X. Control of wide-speed-range operation for a permanent magnet synchronous generator-based wind turbine generator at high wind speeds. *Int. J. Electr. Power Energy Syst.* **2022**, *136*, 107650. [CrossRef]
58. Lebsir, A.; Bentounsi, A.; Benbouzid, M.E.H.; Mangel, H. Electric Generators Fitted to Wind Turbine Systems: An Up-to-Date Comparative Study. In Proceedings of the International Conference on Renewable Energies, Palermo, Italy, 22–25 November 2015. Available online: https://www.researchgate.net/publication/282864467_Electric_Generators_Fitted_to_Wind_Turbine_Systems_An_Up-to-Date_Comparative_Study (accessed on 13 May 2025).
59. Blanco, M.; Navarro, G.; Lafoz, M. Control of power electronics driving a switched reluctance linear generator in wave energy applications. In Proceedings of the 2009 13th European Conference on Power Electronics and Applications, Barcelona, Spain, 8–10 September 2009; pp. 1–9.
60. Whittaker, T.; Folley, M. Nearshore oscillating wave surge converters and the development of Oyster. *Philos. Trans. R. Soc. A Math. Phys. Eng. Sci.* **2012**, *370*, 345–364. [CrossRef] [PubMed]
61. Henderson, R. Design, simulation, and testing of a novel hydraulic power take-off system for the Pelamis wave energy converter. *Renew. Energy* **2006**, *31*, 271–283. [CrossRef]
62. Seabased. The Technology—Seabased Wave Energy. Available online: https://seabased.com/the-technology (accessed on 13 May 2025).
63. HiWave-5 Project. HiWave-5: Advancing Wave Energy Conversion Technology. Available online: https://www.hiwave-5.eu/ (accessed on 13 May 2025).
64. IMechE. CorPower Boosts Electricity Generation in Calm Seas with C4 Wave Energy Device. Available online: https://www.imeche.org/news/news-article/corpower-boosts-electricity-generation-in-calm-seas-with-c4-wave-energy-device (accessed on 13 May 2025).
65. AWS Ocean Energy. Archimedes Waveswing—Subsea Wave Power. Available online: https://awsocean.com/archimedes-waveswing/ (accessed on 13 May 2025).
66. Eco Wave Power. Eco Wave Power—Sustainable Wave Energy. Available online: https://www.ecowavepower.com/ (accessed on 13 May 2025).

67. Wavepiston. Wavepiston—Turning Waves into Energy. Available online: https://wavepiston.dk/ (accessed on 13 May 2025).
68. SHY Project. SHY Project—Sustainable Hydrogen Generation from Renewable Sources. Available online: https://shyproject.eu/ (accessed on 13 May 2025).
69. Carnegie Clean Energy. Carnegie Clean Energy—Wave Energy Solutions. Available online: https://www.carnegiece.com/ (accessed on 13 May 2025).
70. Mocean Energy. Mocean Energy—Innovative Wave Energy Solutions. Available online: https://www.mocean.energy/ (accessed on 13 May 2025).
71. IDOM. Wave Energy Converter. Available online: https://www.idom.com/en/project/wave-energy-converter/ (accessed on 13 May 2025).
72. Ocean Power Technologies. Ocean Power Technologies—Innovative Ocean Energy Solutions. Available online: https://oceanpowertechnologies.com/ (accessed on 13 May 2025).
73. AW-Energy. WaveRoller—Wave Energy Converter. Available online: https://www.offshore-energy.biz/ondep-project-wins-e19m-eu-funding-to-deploy-wave-energy-array-offshore-portugal/ (accessed on 10 December 2025).
74. Maria-Arenas, A.; Garrido, A.J.; Rusu, E.; Garrido, I. Control Strategies Applied to Wave Energy Converters: State of the Art. *Energies* **2019**, *12*, 3115. [CrossRef]
75. Ekström, R.; Ekergård, B.; Leijon, M. Electrical damping of linear generators for wave energy converters—A review. *Renew. Sustain. Energy Rev.* **2015**, *42*, 116–128. [CrossRef]
76. Polinder, H.; van der Pijl, F.F.A.; de Vilder, G.J.; Tavner, P.J. Comparison of direct-drive and geared generator concepts for wind turbines. *IEEE Trans. Energy Convers.* **2006**, *21*, 725–733. [CrossRef]
77. Fraenkel, P. Marine current turbines: Pioneering the development of marine kinetic energy converters. *Proc. Inst. Mech. Eng. Part A J. Power Energy* **2007**, *221*, 159–169. [CrossRef]
78. Bahaj, A.S.; Molland, A.F.; Chaplin, J.R.; Batten, W.M.J. Power and thrust measurements of marine current turbines under various hydrodynamic flow conditions. *Renew. Energy* **2007**, *32*, 407–426. [CrossRef]
79. Zhou, Z.; Knapp, W.; MacEnri, J.; Sorensen, H.C.; Friis Madsen, E.; Masters, I.; Igic, P. Permanent magnet generator control and electrical system configuration for Wave Dragon MW wave energy take-off system. In Proceedings of the 2008 IEEE International Symposium on Industrial Electronics, Cambridge, UK, 30 June–2 July 2008; pp. 1580–1585. [CrossRef]
80. Wu, F.; Ju, P.; Zhang, X.P.; Qin, C.; Peng, G.J.; Huang, H.; Fang, J. Modeling, Control Strategy, and Power Conditioning for Direct-Drive Wave Energy Conversion to Operate with Power Grid. *Proc. IEEE* **2013**, *101*, 925–941. [CrossRef]
81. Prudell, J.; Stoddard, M.; Brekken, T.K.; von Jouanne, A. A novel permanent magnet tubular linear generator for ocean wave energy. In Proceedings of the 2009 IEEE Energy Conversion Congress and Exposition, San Jose, CA, USA, 20–24 September 2009; pp. 3641–3646. [CrossRef]
82. Park, J.S.; Gu, B.G.; Kim, J.R.; Cho, I.H.; Jeong, I.; Lee, J. Active Phase Control for Maximum Power Point Tracking of a Linear Wave Generator. *IEEE Trans. Power Electron.* **2017**, *32*, 7651–7662. [CrossRef]
83. Ramirez, D.; Bartolome, J.P.; Martinez, S.; Herrero, L.C.; Blanco, M. Emulation of an OWC Ocean Energy Plant with PMSG and Irregular Wave Model. *IEEE Trans. Sustain. Energy* **2015**, *6*, 1515–1523. [CrossRef]
84. Zhang, Z.; Zhao, Y.; Qiao, W.; Qu, L. A Discrete-Time Direct Torque Control for Direct-Drive PMSG-Based Wind Energy Conversion Systems. *IEEE Trans. Ind. Appl.* **2015**, *51*, 3504–3514. [CrossRef]
85. Li, W.; Chau, K.T.; Jiang, J.Z. Application of Linear Magnetic Gears for Pseudo-Direct-Drive Oceanic Wave Energy Harvesting. *IEEE Trans. Magn.* **2011**, *47*, 2624–2627. [CrossRef]
86. Prado, M.; Polinder, H. Direct drive in wave energy conversion—AWS full scale prototype case study. In Proceedings of the 2011 IEEE Power and Energy Society General Meeting, Detroit, MI, USA, 24–29 July 2011; pp. 1–7. [CrossRef]
87. Liao, Z.; Sun, T.; Al-Ani, M.; Jordan, L.B.; Li, G.; Wang, Z.; Belmont, M.; Edwards, C.; Zhan, S. Modelling and Control Tank Testing Validation for Attenuator Type Wave Energy Converter—Part II: Linear Noncausal Optimal Control and Deterministic Sea Wave Prediction Tank Testing. *IEEE Trans. Sustain. Energy* **2023**, *14*, 1758–1768. [CrossRef]
88. Xia, T.; Yu, H.; Chen, Z.; Huang, L.; Liu, X.; Hu, M. Design and Analysis of a Field-Modulated Tubular Linear Permanent Magnet Generator for Direct-Drive Wave Energy Conversion. *IEEE Trans. Magn.* **2017**, *53*, 8103904. [CrossRef]
89. Ahamed, R.; McKee, K.; Howard, I. A Review of the Linear Generator Type of Wave Energy Converters' Power Take-Off Systems. *Sustainability* **2022**, *14*, 9936. [CrossRef]
90. Farrok, O.; Islam, M.R.; Islam Sheikh, M.R.; Guo, Y.; Zhu, J.; Lei, G. Oceanic Wave Energy Conversion by a Novel Permanent Magnet Linear Generator Capable of Preventing Demagnetization. *IEEE Trans. Ind. Appl.* **2018**, *54*, 6005–6014. [CrossRef]
91. Attaianese, C.; Carbone, S.; Marignetti, F. Thermal design of linear generators for wave energy converters. In Proceedings of the The XIX International Conference on Electrical Machines—ICEM 2010, Rome, Italy, 6–8 September 2010; pp. 1–8. [CrossRef]

92. Sattarov, R.R.; Ziganshin, T. Axial-Flux Permanent Magnet Synchronous Generator for Float Buoy Type Wave Energy Converters. In Proceedings of the 2019 Dynamics of Systems, Mechanisms and Machines (Dynamics), Omsk, Russia, 5–7 November 2019; pp. 1–6. [CrossRef]
93. Zhao, M.; Zuo, S.; Zhang, H.; Xu, Y.; Zhou, J. Design and Analysis of a Primary Permanent Magnet Transverse Flux Linear Generator for Direct Drive Wave Energy Converters. In Proceedings of the 2021 13th International Symposium on Linear Drives for Industry Applications (LDIA), Wuhan, China, 1–3 July 2021; pp. 1–5. [CrossRef]
94. Xu, L.; Zhu, X.; Zhang, C.; Zhang, L.; Quan, L. Power Oriented Design and Optimization of Dual Stator Linear-Rotary Generator with Halbach PM Array for Ocean Energy Conversion. *IEEE Trans. Energy Convers.* **2021**, *36*, 3414–3426. [CrossRef]
95. Xia, T.; Yu, H.; Guo, R.; Liu, X. Research on the Field-Modulated Tubular Linear Generator with Quasi-Halbach Magnetization for Ocean Wave Energy Conversion. *IEEE Trans. Appl. Supercond.* **2018**, *28*, 5206105. [CrossRef]
96. Zhang, J.; Yu, H.; Hu, M.; Huang, L.; Xia, T. Research on a PM Slotless Linear Generator Based on Magnet Field Analysis Model for Wave Energy Conversion. *IEEE Trans. Magn.* **2017**, *53*, 8208404. [CrossRef]
97. Huang, L.; Chen, M.; Wang, L.; Yue, F.; Guo, R.; Fu, X. Analysis of a Hybrid Field-Modulated Linear Generator For Wave Energy Conversion. *IEEE Trans. Appl. Supercond.* **2018**, *28*, 0601205. [CrossRef]
98. Prudell, J.; Stoddard, M.; Amon, E.; Brekken, T.K.A.; von Jouanne, A. A Permanent-Magnet Tubular Linear Generator for Ocean Wave Energy Conversion. *IEEE Trans. Ind. Appl.* **2010**, *46*, 2392–2400. [CrossRef]
99. Jafari, R.; Asef, P.; Ardebili, M.; Derakhshani, M.M. Linear Permanent Magnet Vernier Generators for Wave Energy Applications: Analysis, Challenges, and Opportunities. *Sustainability* **2022**, *14*, 912. [CrossRef]
100. Zhou, Y.; Gao, Y.; Qu, R.; Cheng, Y.; Shi, C. A Novel Dual-Stator HTS Linear Vernier Generator for Direct Drive Marine Wave Energy Conversion. *IEEE Trans. Appl. Supercond.* **2019**, *29*, 5201806. [CrossRef]
101. Zhao, L.; Lu, Q. A Novel Tubular Partitioned Stator Flux-Reversal Permanent Magnet Linear Machine for Direct-Drive Wave Energy Generation. *IEEE Trans. Magn.* **2019**, *55*, 7502707. [CrossRef]
102. Shuraiji, A.L.; Zhu, Z.; Lu, Q. A novel partitioned stator flux reversal permanent magnet linear machine. In Proceedings of the 2015 Tenth International Conference on Ecological Vehicles and Renewable Energies (EVER), Monte-Carlo, Monaco, 31 March–2 April 2015; pp. 1–8. [CrossRef]
103. Huang, L.; Yu, H.; Hu, M.; Zhao, J.; Cheng, Z. A Novel Flux-Switching Permanent-Magnet Linear Generator for Wave Energy Extraction Application. *IEEE Trans. Magn.* **2011**, *47*, 1034–1037. [CrossRef]
104. Ghaheri, A.; Afjei, E.; Torkaman, H. Design optimization of a novel linear transverse flux switching permanent magnet generator for direct drive wave energy conversion. *Renew. Energy* **2022**, *198*, 851–860. [CrossRef]
105. Yang, J.; Huang, L.; Hu, M.; Yu, H.; Jiu, C.; Zhao, D. Research on a control strategy of the flux-switching permanent magnet linear generator for wave energy extraction. In Proceedings of the 2015 18th International Conference on Electrical Machines and Systems (ICEMS), Pattaya, Thailand, 25–28 October 2015; pp. 1666–1670. [CrossRef]
106. Liu, C.; Dong, R.; lin Ye, B. Comprehensive sensitivity analysis and multi-objective optimization on a permanent magnet linear generator for wave energy conversion. *Renew. Energy* **2022**, *198*, 841–850. [CrossRef]
107. Zhang, J.; Yu, H.; Chen, Q.; Hu, M.; Huang, L.; Liu, Q. Design and Experimental Analysis of AC Linear Generator with Halbach PM Arrays for Direct-Drive Wave Energy Conversion. *IEEE Trans. Appl. Supercond.* **2014**, *24*, 0502704. [CrossRef]
108. Johnson, M.; Gardner, M.C.; Toliyat, H.A.; Englebretson, S.; Ouyang, W.; Tschida, C. Design, Construction, and Analysis of a Large-Scale Inner Stator Radial Flux Magnetically Geared Generator for Wave Energy Conversion. *IEEE Trans. Ind. Appl.* **2018**, *54*, 3305–3314. [CrossRef]
109. Said, H.A.; García-Violini, D.; Ringwood, J.V. Wave-to-Grid (W2G) control of a wave energy converter. *Energy Convers. Manag. X* **2022**, *14*, 100190. [CrossRef]
110. Cummins, W.E. The Impulse Response Function and Ship Motions. Technical Report DTMB Report 1661, David Taylor Model Basin. 1962. Available online: https://dome.mit.edu/bitstream/handle/1721.3/49049/DTMB_1962_1661.pdf (accessed on 13 May 2025).
111. Davidson, J.; Giorgi, S.; Ringwood, J. Identification of Wave Energy Device Models From Numerical Wave Tank Data—Part 1: Numerical Wave Tank Identification Tests. *IEEE Trans. Sustain. Energy* **2016**, *7*, 1012–1019. [CrossRef]
112. Falnes, J. *Ocean Waves and Oscillating Systems: Linear Interactions Including Wave-Energy Extraction*; Cambridge University Press: Cambridge, UK, 2002.
113. Rogne, Ø.Y. Numerical and Experimental Investigation of a Hinged 5-Body Wave Energy Converter. Ph.D. Thesis, Norwegian University of Science and Technology, Trondheim, NO, USA, 2014.
114. Li, L.; Wang, H.; Gao, Y. Development of a Real-Time Latching Control Algorithm Based on Wave Force Prediction. *IEEE J. Ocean. Eng.* **2021**, *46*, 583–593. [CrossRef]

115. Sullivan, A.C.M.O.; Lightbody, G. Predictive control of a wave to wire energy conversion system—The importance of field weakening. In Proceedings of the 2016 UKACC 11th International Conference on Control (CONTROL), Belfast, UK, 31 August–2 September 2016; pp. 1–6. [CrossRef]
116. Kumar, A.; Kumar, A.; Kumar, C.; Kasari, P.R.; Das, B.; Chakrabarti, A. MMCC based PMSG for Oceanic Wave Energy Conversion System. In Proceedings of the 2020 IEEE International Conference on Power Electronics, Drives and Energy Systems (PEDES), Jaipur, India, 16–19 December 2020; pp. 1–6. [CrossRef]
117. Rosati, M.; Henriques, J.C.C.; Ringwood, J.V. Oscillating-water-column wave energy converters: A critical review of numerical modelling and control. *Energy Convers. Manag. X* **2022**, *16*, 100322. [CrossRef]
118. El-Saady, G.; Ibrahim, E.N.; Ziedan, H.; Elsayed, M. Analysis of Wind Turbine Driven Permanent Magnet Synchronous Generator under Different Loading Conditions. *Int. J. Technol. Educ. Sci.* **2013**, *4*, 97–111.
119. Lim, K.C.; Woo, J.K.; Kang, G.H.; Hong, J.P.; Kim, G.T. Detent Force Minimization Techniques in Permanent Magnet Linear Synchronous Motors. *IEEE Trans. Magn.* **2002**, *38*, 1157–1160. [CrossRef]
120. Shu, S.; Zhang, Y.; Wang, X.; Pan, Q.; Tao, X. Space Vector Control of a Permanent Magnet Linear Synchronous Motor Based on the Improved Single Neuron PID Algorithm. *Control Eng. Appl. Inform.* **2020**, *22*, 74–84.
121. Wang, X.; Chen, F.; Zhu, R.; Huang, X.; Sang, N.; Yang, G.; Zhang, C. A Review on Disturbance Analysis and Suppression for Permanent Magnet Linear Synchronous Motor. *Actuators* **2021**, *10*, 77. [CrossRef]
122. Galea, M.; Buticchi, G.; Empringham, L.; De Lillo, L.; Gerada, C. Design of a High-Force-Density Tubular Motor. *IEEE Trans. Ind. Appl.* **2014**, *50*, 2523–2532. [CrossRef]
123. Cupertino, F.; Giangrande, P.; Pellegrino, G.; Salvatore, L. End Effects in Linear Tubular Motors and Compensated Position Sensorless Control Based on Pulsating Voltage Injection. *IEEE Trans. Ind. Electron.* **2011**, *58*, 494–502. [CrossRef]
124. Parviainen, A. Design of Axial-Flux Permanent-Magnet Low-Speed Machines and Performance Comparison Between Radial-Flux and Axial-Flux Machines. Ph.D. Thesis, Lappeenranta University of Technology, Lappeenranta, Finland, 2004.
125. Zhao, J.; Liu, X.; Wang, S.; Zheng, L. Review of Design and Control Optimization of Axial Flux PMSM in Renewable-Energy Applications. *Chin. J. Mech. Eng.* **2023**, *36*, 45. [CrossRef]
126. Sabah, N.; Humod, A.T.; Hasan, F.A. Field Oriented Control of the Axial Flux PMSM Based on Multi-Objective Particle Swarm Optimization. *J. Eng. Appl. Sci. Kansai Univ. Rep.* **2020**, *62*, 1493.
127. Kumar, R.; Zhu, Z.Q.; Duke, A.; Thomas, A.; Clark, R.; Azar, Z.; Wu, Z.Y. A Review on Transverse Flux Permanent Magnet Machines for Wind Power Applications. *IEEE Access* **2020**, *8*, 216543–216565. [CrossRef]
128. Ballestín-Bernad, V.; Artal-Sevil, J.S.; Domínguez-Navarro, J.A. A Review of Transverse Flux Machines Topologies and Design *Energies* **2021**, *14*, 7173. [CrossRef]
129. Cui, Y.; Zhang, Y.; Yin, Z.; Bai, C. Modeling and Vector-Control Strategy of a Transverse Flux Permanent Magnet Machine. In Proceedings of the International Conference on Power Systems Technology (POWERCON), Pune, India, 21–23 December 2017.
130. Zulkarnain, N.F.; Ibrahim, T.; Romlie, M.F. Analysis of Radial and Halbach Permanent Magnet Arrangements for Ceiling Fan applications. *Int. J. Adv. Sci. Eng. Inf. Technol.* 2018, *22*, 1–6.
131. Zhu, Z.Q.; Xia, Z.P.; Shi, Y.F.; Howe, D.; Pride, A.; Chen, X.J. Performance of Halbach Magnetized Brushless AC Motors. *IEEE Trans. Magn.* **2003**, *39*, 2992–2994. [CrossRef]
132. Wu, W.; El-Refaie, A.M. Permanent Magnet Vernier Machines: A Review. In Proceedings of the 2018 XIII International Conference on Electrical Machines (ICEM), Alexandroupoli, Greece, 3–6 September 2018.
133. Fu, W.N.; Ho, S.L. A Quantitative Comparative Analysis of a Novel Flux-Modulated Permanent Magnet Motor for Low-Speed Drive. *IEEE Trans. Magn.* **2010**, *46*, 127–134. [CrossRef]
134. Xiang, J.; Wei, J.; Zhu, X. Torque Ripple Suppression of a PM Vernier Machine from the Perspective of Time and Space Harmonic Magnetic Field. *IEEE Trans. Ind. Electron.* **2024**, *71*, 10150–10161. [CrossRef]
135. Wang, Q.; Zhao, X.; Niu, S. Flux-Modulated Permanent Magnet Machines: Challenges and Opportunities. *World Electr. Veh. J.* **2021**, *12*, 13. [CrossRef]
136. Xu, G.; Jian, L.; Gong, W.; Zhao, W. Quantitative Comparison of Flux-Modulated Interior Permanent Magnet Machines. *Prog. Electromagn. Res.* **2012**, *125*, 247–269. [CrossRef]
137. Xia, C.; Li, D.; Qu, R.; Li, J. Design Procedure of Flux Reversal Permanent Magnet Machines. *IEEE Trans. Ind. Appl.* **2016**, *52*, 4049–4059. [CrossRef]
138. Zhu, X.; Hua, W. Stator-Slot/Rotor-Pole Pair Combinations of Flux-Reversal Permanent Magnet Machines. *IEEE Trans. Ind. Electron.* **2017**, *64*, 9873–9884. [CrossRef]
139. Hua, W.; Huang, W.; Yu, F. Improved Model-Predictive-Flux-Control Strategy for Three-Phase Four-Switch Inverter-Fed Flux-Reversal Permanent Magnet Machine Drives. *IET Electr. Power Appl.* **2017**, *11*, 717–728. [CrossRef]

140. Zhu, Z.Q.; Hua, W.; Cheng, M.; Howe, D. Switched Flux Permanent Magnet Machines—Innovation Continues. *IEEE Trans. Ind. Electron.* **2012**, *58*, 543–552. [CrossRef]
141. Zhu, X.; Hua, W.; Yu, F. Cogging Torque Minimisation in FSPM Machines by Right-Angle-Shaped Stator Teeth. *IET Electr. Power Appl.* **2018**, *12*, 331–338. [CrossRef]
142. Huang, W.; Hua, W.; Yu, F. A Model Predictive Current Control of Flux-Switching Permanent Magnet Machines for Torque Ripple Minimization. *AIP Adv.* **2017**, *7*, 056609. [CrossRef]
143. Merlyn, J.O.; Lenin, N.C. Review of Control Topologies for Flux Switching Motor. *Majlesi J. Energy Manag.* **2023**, *11*, 51241–51259. [CrossRef]
144. Lim, S. Sensorless-FOC with Flux-Weakening and MTPA for IPMSM Motor Drives. Available online: https://www.ti.com/lit/an/spracf3/spracf3.pdf?ts=1766445446192 (accessed on 13 May 2025).
145. Ammar, R.; Trabelsi, M.; Mimouni, M.F.; Ben Ahmed, H.; Benbouzid, M. Flux weakening control of PMSG based on direct wave energy converter systems. In Proceedings of the 2017 International Conference on Green Energy Conversion Systems (GECS), Hammamet, Tunisia, 23–25 March 2017; pp. 1–7. [CrossRef]
146. Huang, W.; Yang, J. A Novel Piecewise Velocity Control Method Using Passivity-Based Controller for Wave Energy Conversion. *IEEE Access* **2020**, *8*, 59029–59043. [CrossRef]
147. Zhu, L.; Yao, Z.; Li, W. A Real-Time Maximum Power Points Tracking Strategy Consider Power-to-Average Ratio Limiting for Wave Energy Converter. *IEEE Access* **2022**, *10*, 48039–48048. [CrossRef]
148. Jasinski, M. Vector Control of AC/DC/AC Converter—Generator Subset in Wave-to-Wire Power Train for Wave Dragon MW. In Proceedings of the EUROCON 2007—The International Conference on "Computer as a Tool", Warsaw, Poland, 9–12 September 2007; pp. 1324–1327. [CrossRef]
149. Tom, N.; Yeung, R.W. Experimental Confirmation of Nonlinear-Model- Predictive Control Applied Offline to a Permanent Magnet Linear Generator for Ocean-Wave Energy Conversion. *IEEE J. Ocean. Eng.* **2016**, *41*, 281–295. [CrossRef]
150. Luckins, A.; Duttagupta, S.P. Model predictive control strategy for direct drive PMSG and DFIG for ocean wave energy converter system. In Proceedings of the OCEANS 2016 MTS/IEEE Monterey, Monterey, CA, USA, 19–23 September 2016; pp. 1–4. [CrossRef]
151. Huang, Z.; Wei, Q.; Xiao, X.; Xia, Y.; Rivera, M.; Wheeler, P. Enhanced Dual–Vector Model Predictive Control for PMSM Drives Using the Optimal Vector Selection Principle. *Energies* **2023**, *16*, 7482. [CrossRef]
152. Zarei, M.E.; Ramirez, D.; Veganzones, C.; Rodríguez, J. Predictive Direct Control of SPMS Generators Applied to the Machine Side Converter of an OWC Power Plant. *IEEE Trans. Power Electron.* **2020**, *35*, 6719–6731. [CrossRef]
153. Mortazavizadeh, S.A.; Yazdanpanah, R.; Gaona, D.C.; Anaya-Lara, O. Fault diagnosis and condition monitoring in wave energy converters: A review. *Energies* **2023**, *16*, 6777. [CrossRef]
154. Zhang, Y.; Zeng, T.; Gao, Z. Fault diagnosis and fault-tolerant control of energy maximization for wave energy converters. *IEEE Trans. Sustain. Energy* **2022**, *13*, 1771–1778. [CrossRef]
155. Zadeh, L.G.; Brekken, T.K.A.; Fern, A.; Shahbaz, A.H. Hardware in the loop wave energy converter control under control faults and model mismatch. *IEEE Trans. Sustain. Energy* **2023**, *15*, 13–22. [CrossRef]
156. Papini, G.; Faedo, N.; Mattiazzo, G. Fault diagnosis and fault-tolerant control in wave energy: A perspective. *Renew. Sustain. Energy Rev.* **2024**, *199*, 114507. [CrossRef]
157. González-Esculpi, A.; Verde, C.; Maya-Ortiz, P. Fault-tolerant control for a wave energy converter by damping injection. In Proceedings of the IEEE Conference on Control Technology and Applications (CCTA), San Diego, CA, USA, 8–11 August 2021; pp. 673–678. [CrossRef]
158. Ramirez, D.; Blanco, M.; Zarei, M.E.; Gupta, M. Robust control of a floating OWC WEC under open-switch fault condition in one or in both VSCs. *IET Renew. Power Gener.* **2020**, *14*, 2538–2549. [CrossRef]